

TeraHertz Band Communication: An Old Problem Revisited and Research Directions for the Next Decade

Ian F. Akyildiz, *Life Fellow, IEEE*, Chong Han, *Member, IEEE*, Zhifeng Hu, Shuai Nie, *Member, IEEE*, and Josep M. Jornet, *Senior Member, IEEE*

Abstract—TeraHertz (THz) band communications are envisioned as a key technology for 6G and Beyond. As a fundamental wireless infrastructure, THz communication can boost abundant promising applications. In 2014, our team published two comprehensive roadmaps for the development and progress of THz communication networks [1], [2], which helped the research community to start research on this subject afterwards. In particular, this topic became very important and appealing to the research community due to 6G wireless systems design and development in recent years. Many papers are getting published covering different aspects of wireless systems using the THz band. With this paper, our aim is looking back to the last decade and revisiting the old problems and pointing out what has been achieved in the research community so far. Furthermore, in this paper still to be investigated new research challenges for the THz band communication systems are presented by covering diverse subtopics such as from perspectives of devices, channel behavior, communication and networking problems, physical testbeds and demonstration systems. The key aspects presented in this paper will enable THz communications as a pillar of 6G and Beyond wireless systems in the next decade.

Index Terms—TeraHertz communications, 6G and Beyond wireless systems, Distance limitations, TeraHertz devices, TeraHertz testbeds, Propagation modeling, TeraHertz networks.

I. INTRODUCTION

TeraHertz (THz) Band (0.1–10 THz) communications is envisioned as one of the key enabling technologies to satisfy the exponential growth of data traffic volume accompanied by the demand for higher data rates and better coverage in 6G and Beyond wireless systems. As shown in Fig. 1, 6G wireless systems are expected to support peak data rates of 1 Tbps, where the peak spectral efficiency is expected to be 60 bps/Hz, end-to-end reliability in terms of packet error rates of 10^{-9} , and end-to-end latency of 0.1 ms. Furthermore, the energy efficiency will be improved 100 times better than in 5G, as well as 1 to 3 mm sensing resolutions in the next generation Internet of Things with ultra-massive number of devices, e.g., on a scale of tens of billions [1]–[6].

Millimeter-wave (mm-wave) communications (30–300 GHz) under 100 GHz have been officially adopted in

recent 5G cellular systems. While the trend for higher carrier frequencies is apparent, it is still difficult for mm-wave systems to support Tbps data rates as well as the above mentioned strict Quality of Service requirements. Limited by the total consecutive available bandwidth of less than 10 GHz in the mm-wave systems under 100 GHz, the spectrum efficiency is required to reach 100 bps/Hz, which is unprecedentedly challenging even with advanced physical-layer techniques. THz band reveals its potential as one of key wireless technologies to fulfill the future demands for 6G wireless systems, thanks to its four strengths: 1) from tens and up to hundreds of GHz of contiguous bandwidth, 2) picosecond-level symbol duration, 3) integration of thousands of sub-millimeter-long antennas, 4) ease of coexistence with other regulated and standardized spectrum. The THz band has traditionally been one of the least explored frequency bands in the electromagnetic (EM) spectrum, mostly due to the lack of efficient and practical THz transceivers and antennas. Nevertheless, practical THz communication systems are being enabled by the major progress in the last ten years to expedite the way of fulfilling this gap [7]–[9].

With the multi-GHz bandwidth, the THz spectrum is favored as a candidate to resolve the spectrum scarcity problem and tremendously enhance the capacity of current wireless systems [10]. In addition to the promised Tbps-level links for cellular systems, THz-band spectrum can also be utilized in many use cases, such as Tbps WLAN system (*Tera-WiFi*), Tbps Internet-of-Things (*Tera-IoT*) in wireless data centers, Tbps integrated access backhaul (*Tera-IAB*) wireless networks, and ultra-broadband THz space communications (*Tera-SpaceCom*), as illustrated in Fig. 2. Besides macro/micro-scale applications, motivated by the state-of-the-art nanoscale transceivers and antennas that intrinsically operate in the THz band, further use cases include wireless networks-on-chip communications (WiNoC) as well as wireless connections in networks of nanomachines such as in Internet of NanoThings (IoNT) [11], shown in Fig. 3 where these nano-devices can be the building block for the intra-body communications [12], [13] to provide advanced healthcare services. To further integrate sensing and communication (ISAC), also known as joint communication and sensing (JCS) capabilities, the promising applications, containing THz virtual/augmented reality (VR/AR), vehicular communication and radar sensing, and millimeter-level indoor localization, are shown in Fig. 4 [14]. Moreover, powerful deep learning (DL) schemes can further enable THz holographic, haptic and telepresence communication, or metaverse, to offer a more intuitive visual and aesthetic experience for entertainment, academic research,

Ian F. Akyildiz is with Truva Inc., Alpharetta, GA 30022, USA (email: ian@truvainc.com).

Chong Han and Zhifeng Hu are with the Terahertz Wireless Communications (TWC) Laboratory, Shanghai Jiao Tong University, Shanghai 200240, China (email: {chong.han, zhifeng.hu}@sjtu.edu.cn).

Shuai Nie is with the School of Computing, University of Nebraska-Lincoln, Lincoln, NE 68588, USA (email: shuainie@unl.edu).

Josep M. Jornet is with the Ultrabroadband Nanonetworking Laboratory, Institute for the Wireless Internet of Things, Department of Electrical and Computer Engineering, Northeastern University, Boston, MA 02215, USA (email: jmjornet@northeastern.edu).

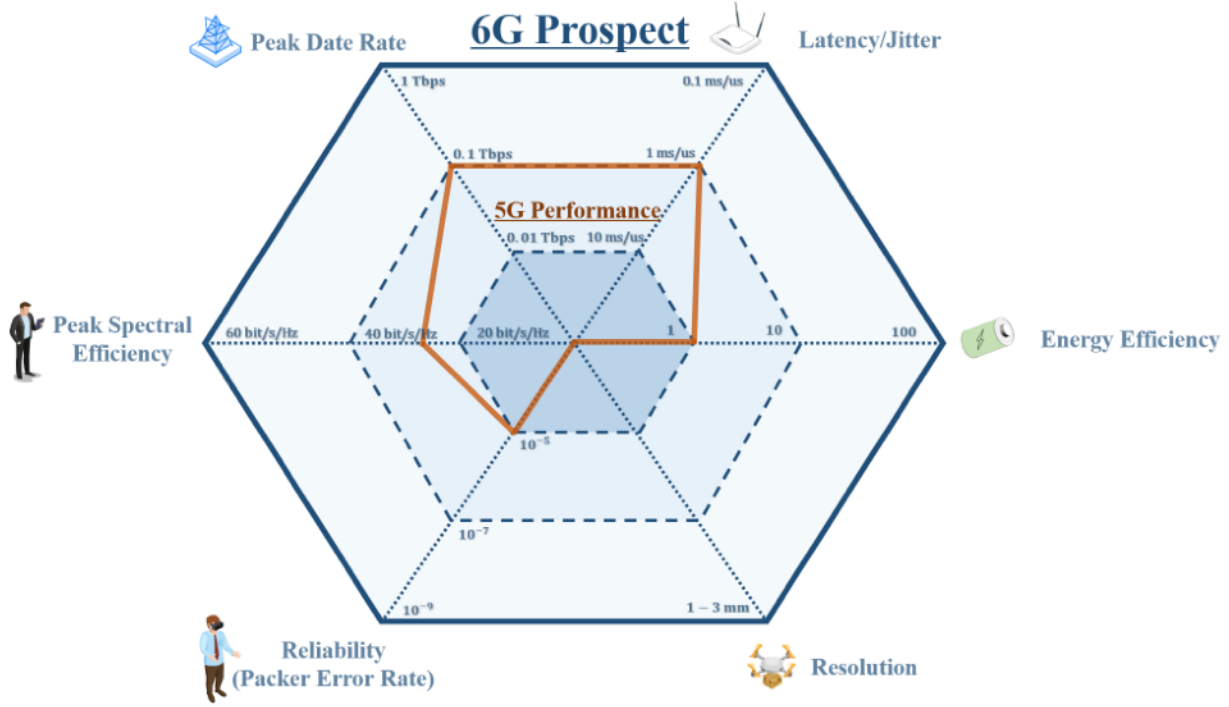


Fig. 1. Performance objectives for 6G.

and so on.

The road to close the THz gap and realize THz communications needs to be paved by the communication community jointly. In this direction, in 2019, the FCC (Federal Communication Commission) created a new category of experimental licenses and allocated over 20 GHz of unlicensed spectrum between 95 GHz and 3 THz, to facilitate the testing of 6G and Beyond technologies, including those funded by multiple NSF and Department of Defense (DoD) grants as well as industry driven efforts.

Global research activities are ongoing as well, including Europe Horizon 2020 and key programs funded by Chinese Ministry of Science and Technology [15]. Also the standardization activities are on the way since the last several years. The first wireless communications standard, IEEE 802.15.3d (WPAN), was published in 2017, which operates at the 300 GHz frequency range to support 100 Gbps and above wireless point-to-point links [16]. In November 2019, ITU-R WRC-19 Agenda Item 1.15 identified in total 137 GHz bandwidth for land mobile and fixed services, covering the spectrum bands over 0.275–0.296 THz, 0.306–0.313 THz, 0.318–0.333 THz, and 0.356–0.45 THz [17]. More recently, in July 2021, the IEEE Communications Society (ComSoc) Radio Communications Committee (RCC) Special Interest Group (SIG) on THz communications has been established, with the objectives and missions to advance the research and development of THz communications in 6G and Beyond [18].

In 2014, we published two comprehensive roadmap papers for the development of THz communication networks [1], [2], which helped the research community to pay attention to this upcoming important subject. In particular, many people started research on this topic and the subject became like a wildfire

with hundreds of papers getting published in recent years. With this paper, we want to look back at the last decade and revisit the old problems and point out what has been achieved in the research community. Furthermore, we look into the next decade and point out all the remaining research problems so that THz Band wireless communication can be fully utilized. More specifically, our main contributions are summarized as follows.

- We present the development of pathways for THz devices, including analog front-ends, reconfigurable antenna systems and ultra-broadband digital back ends.
- We provide a thorough inspection on THz channels, containing measurement methods, modeling schemes, unique propagation properties, and link budget analysis.
- In light of the device and channel characteristics, we conduct a detailed review of the THz physical-layer technologies, including modulation, coding, dynamic hybrid beamforming, beam estimation and tracking, synchronization, localization, as well as physical layer security.
- Looking up to higher-layer networking protocols, we inspect the medium access control layer, interference and coverage, multi-hop communications, together with the routing and scheduling approaches in THz wireless communication systems.
- We also present the advancement of THz experimental and simulation testbeds.
- We discuss the open problems and present potential future research directions from all the aforementioned aspects of THz communications for the next decade.

Throughout the paper, we highlight, discuss, and address the grand challenge in THz communications: the limited commu-

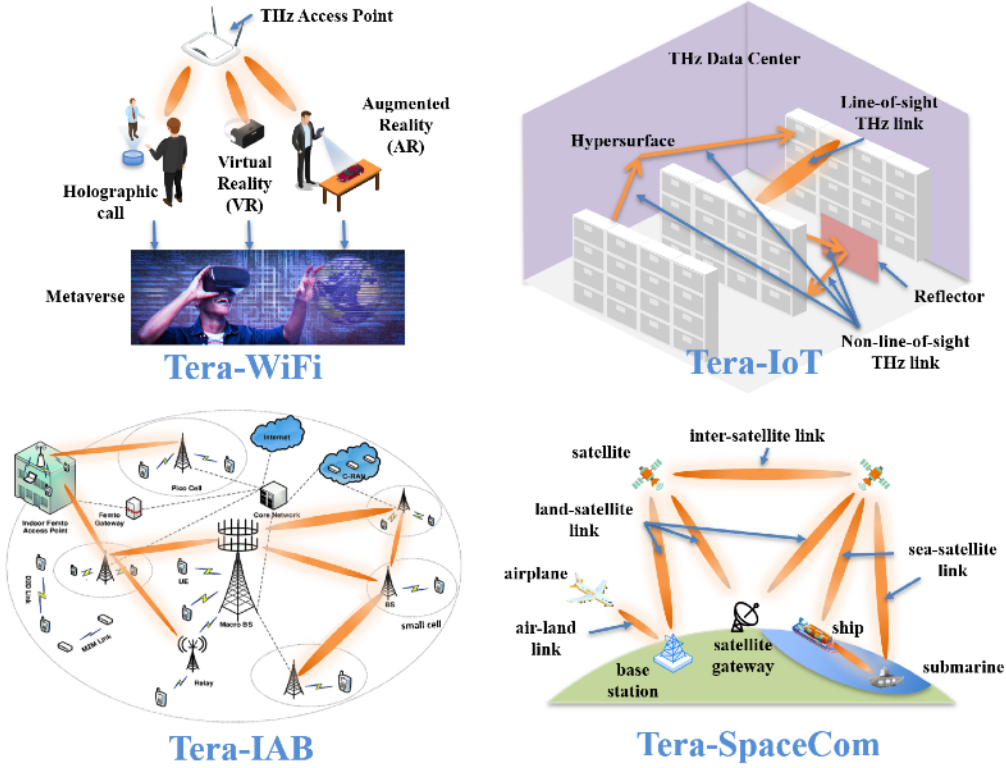


Fig. 2. 6G applications enabled by THz communications, including Tbps WLAN system (*Tera-WiFi*), Tbps Internet-of-Things (*Tera-IoT*) in wireless data center, Tbps integrated access and backhaul (*Tera-IAB*) wireless networks, and ultra-broadband THz space communications (*Tera-SpaceCom*).

nication distance resulting from a combination of the physics of the wireless channel and the physics of THz devices. On the one hand, very high free-space propagation loss, diffusely scattering, vulnerability to line-of-sight (LoS) blockage, and molecular absorption loss impose channel degradation of the THz spectrum. On the other hand, limited transmit power and reduced receiver sensitivity downgrade the signal strength. The THz device technology is investigated in Sec. III, and the THz channel is analyzed in Sec. IV, which will highlight the distance problem. In our prior work [19], four directions to tackle the crucial problem of distance limitation are investigated, including distance-aware physical layer design, ultra-massive MIMO communication, reflectarrays, and intelligent surfaces. In this work, we will present the solutions to overcome this problem, ranging from physical-layer functionalities in Sec. V, higher-layer networking protocols in Sec. VI, to experimental and simulation testbeds in Sec. VII. The organization of this work is illustrated in Fig. 5.

II. RELATED WORK

In recent years, the publications on THz band reached a peak where not only technical papers are being published but also many tutorials and review papers are appearing in the literature. In this section, we give a global view of all these publications in Table I. Note that if any important paper is missing, it is not intentional and we apologize ahead of time.

Different research directions are highlighted in these works, including five main aspects, namely, hardware for THz communications [1], [2], [4], [5], [21], [23]–[25], [28], [29],

[33], THz channels [1], [2], [4], [5], [20], [21], [23], [26], [29]–[31], THz communication techniques [1], [2], [4], [5], [27], [30]–[32], THz networking [1], [2], [31], [32], and THz experimental and simulation testbeds [1], [2].

Furthermore, the number of articles surveying THz communications raised remarkably after 2017, suggesting the ceaseless increase of research attention to this untapped potential band recently. A holistic review of the THz communications that covers all the classical and novel research directions is hence motivated. In contrast to most of the existing related works, a thorough inspection of THz wireless communications is presented in this paper, containing THz devices, channels, communication techniques, networking, and testbed. Although all these aspects were covered in [1], [2], relevant work was scarce before 2014, especially about THz networking and testbeds. However, owing to the fast development of THz communications, more and more creative and influential solutions arise. In this article, we revisit all the most recent research publications about THz communications, based on which the innovative open issues and potential future research directions are proposed.

III. TERAHERTZ DEVICE TECHNOLOGY

Traditionally, the lack of compact energy-efficient high-power THz transmitters and low-noise high-sensitivity receivers has limited the practical use of the THz band for communication systems. Fortunately, the so-called THz technology gap has been significantly closed in the last decade thanks

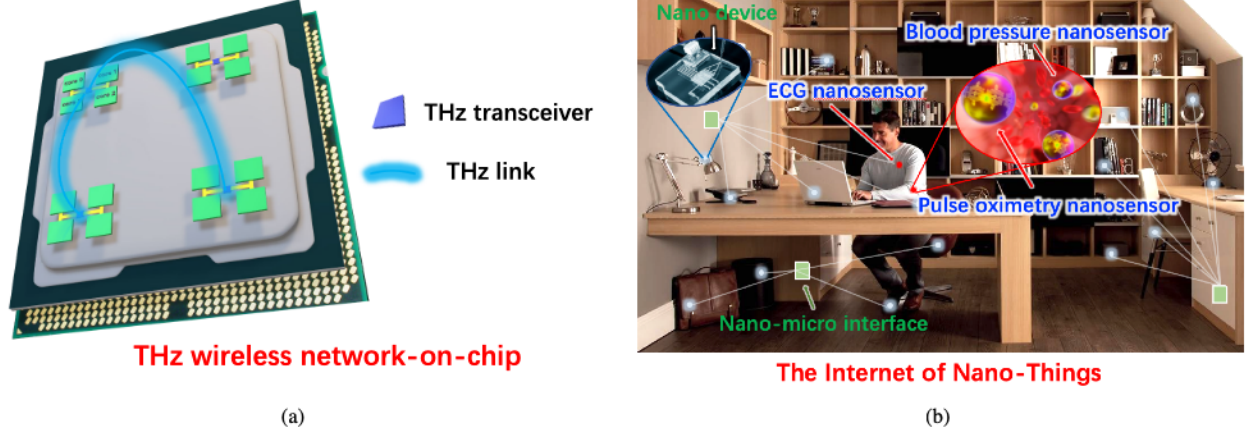


Fig. 3. Nanoscale applications enabled by THz-band communications, including (a) wireless networks-on-chip communications (WiNoC), and (b) the Internet of Nano-Things (IoNT).

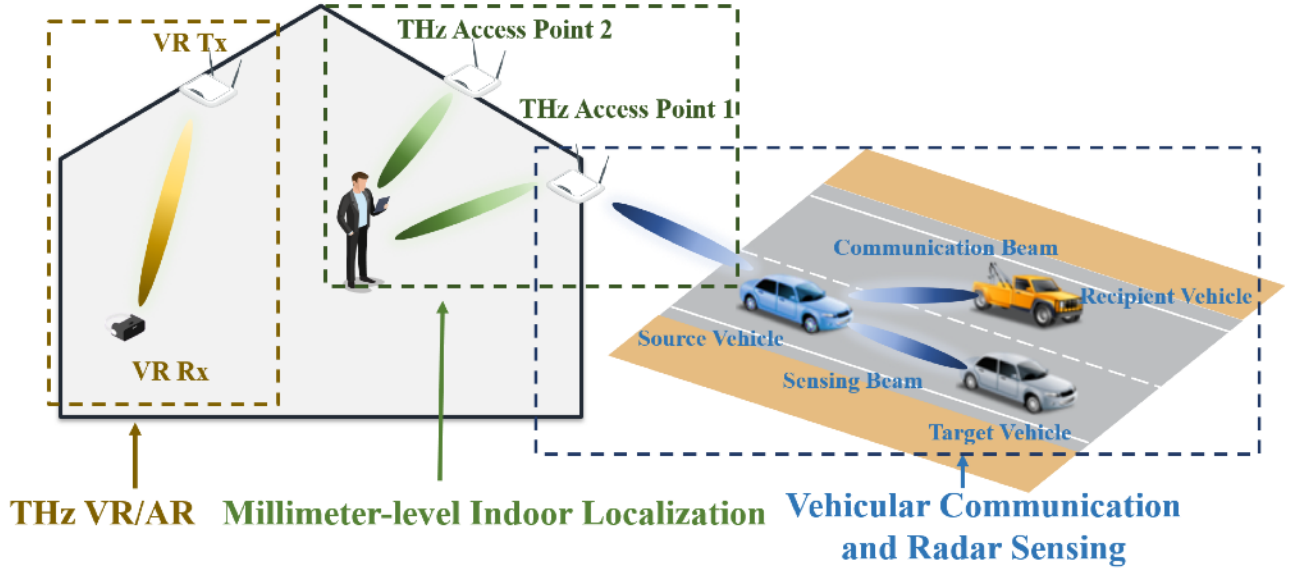


Fig. 4. THz integrated sensing and communication applications.

to major advancement in semiconductor technologies and the development of new materials.

In this section, we first describe the key hardware blocks of a THz wireless system, namely, analog front-ends, antenna systems and digital back-ends, and list the key performance metrics. Then, we review the state of the art and open challenges for each building block.

A. Hardware Building Blocks

The hardware building blocks of a THz wireless communication and sensing system include the analog front-ends, the antenna systems, and the digital back-ends:

- The **analog front-end** at the transmitter is in charge of generating a THz carrier signal or pulse-based waveform, modulating the signal according to the information to be transmitted, amplifying the signal power, and filtering out-of-band emissions (e.g., harmonics) prior to radiation.

Reciprocally, the analog front-end at the receiver is in charge of detecting a THz signal, filtering the out-of-band noise, amplifying the useful signal and recovering the information. The key performance metrics of a front-end include the frequency bands of operation, modulation bandwidth, transmission power, receiver sensitivity, and amplitude and phase noise.

- The **antenna system** is in charge of converting on-chip modulated THz signals at the transmitter front-end into free-space propagating EM signals and, reciprocally, at the receiver, coupling free-space radiation onto the on-chip front-ends. The antenna system can be integrated by one or more antennas, in combination with lenses or reflecting structures. The key performance metrics of an antenna system includes radiation efficiency, directivity gain and beamwidth.
- The **digital back-end** is in charge of generating the con-

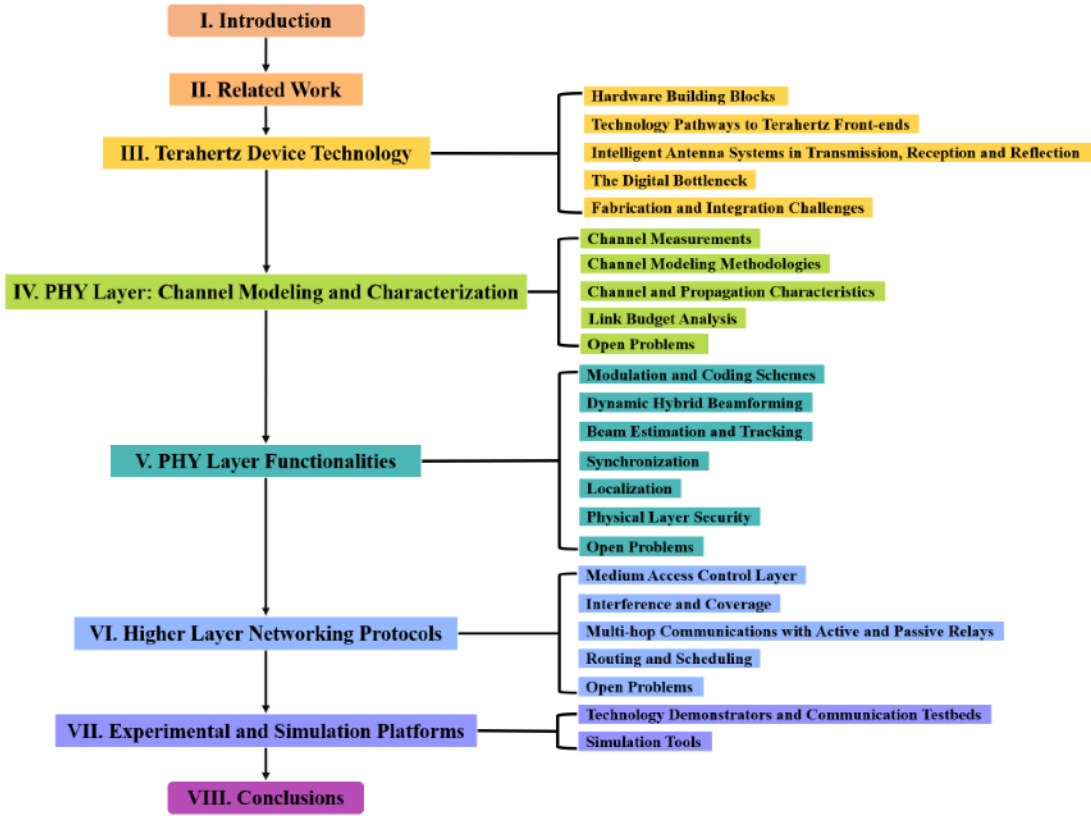


Fig. 5. The structure of this paper.

control signals for the analog front-ends, digitally processing the information signals to be transmitted and received through the analog front-ends and, ultimately, serving as an interface between digital computing devices and the analog wireless channel. The main elements of the digital back-end are the digital to analog converters (DACs) at the transmitter and analog to digital converters (ADCs) at the receiver. Their key performance metrics include the sampling frequency and the sampling resolution.

To unleash the potential of the THz spectrum, a THz communication system should be able to operate at one or more frequency windows within the THz band, with modulation bandwidths in excess of 10 GHz at very least (i.e., two orders of magnitude more than in current 5G systems), a combination of transmission power, antenna gains, and receiver sensitivity that meets the link budget requirements according to the propagation conditions and the targeted communication distance (Sec. IV-D), and with low amplitude and phase noise powers. High power efficiency, low energy consumption and reconfigurability are also critical to the development of intelligent, dynamic and sustainable THz communication and sensing systems for 6G and Beyond.

B. Technology Pathways to Terahertz Front-ends

There are currently three main technology pathways or approaches to the development of THz systems, namely, the electronic, the photonic and the plasmonic approach (Fig. 6). Next, we summarize the state of the art for each approach.

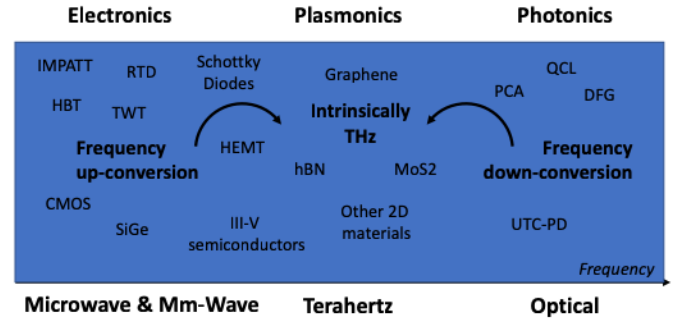


Fig. 6. Technology pathways to THz front-ends.

1) *Electronic Approach*: The goal of this approach is to push the limits of existing technologies for microwave and mm-wave devices to enable THz systems. Besides Resonant Tunneling Diodes (RTDs) [34], [35], IMPact ionization Avalanche Transit Time (IMPATT) diodes [36], [37], and Traveling Wave Tubes (TWTs) [38], [39], the most common technique to generate a THz carrier signal in an electronic approach is the use of **frequency multiplying chains to up-convert a lower-frequency signal** (generally from the microwave and millimeter-wave band). Frequency multiplying chains are integrated by concatenated frequency doublers and/or triplers and are generally followed by a broadband mixer in a heterodyne architecture. The same architecture can be used reciprocally at the receiver to down-convert

TABLE I
RELATED TUTORIALS, SURVEYS AND MAGAZINES.

Title and Reference	Year	Component					
		Device	Channel	PHY Layer	Functionality	Network	Testbed
Short-Range Ultra-Broadband Terahertz Communications: Concepts and Perspectives [20]	2007		✓				
Review of Terahertz and Subterahertz Wireless Communications [21]	2010	✓	✓				
Terahertz Terabit Wireless Communication [22]	2011	✓					
Present and Future of Terahertz Communications [23]	2011	✓	✓				
TeraNets: Ultra-broadband Communication Networks in the Terahertz Band [2]	2014	✓	✓		✓	✓	✓
Terahertz Band: Next Frontier for Wireless Communications [1]	2014	✓	✓		✓	✓	✓
Advances in Terahertz Communications Accelerated by Photonics [24]	2016	✓					
THz Diode Technology: Status, Prospects, and Applications [25]	2017	✓					
Propagation Modeling for Wireless Communications in the Terahertz Band [26]	2018		✓				
Tutorial: Terahertz Beamforming, from Concepts to Realizations [27]	2018				✓		
Terahertz Integrated Electronic and Hybrid Electronic–Photonic Systems [28]	2018	✓					
Wireless Communications and Applications above 100 GHz: Opportunities and Challenges for 6G and Beyond [5]	2019		✓		✓		
Terahertz Band: The Last Piece of RF Spectrum Puzzle for Communication Systems [4]	2019	✓	✓		✓		
Wave Propagation and Channel Modeling in Chip-Scale Wireless Communications: A Survey from Millimeter-Wave to Terahertz and Optics [29]	2019	✓	✓				
A Holistic Investigation of Terahertz Propagation and Channel Modeling toward Vertical Heterogeneous Networks [30]	2020		✓		✓	✓	
Beyond 100 Gb/s Optoelectronic Terahertz Communications: Key Technologies and Directions [31]	2020	✓			✓		
Toward End-to-End, Full-Stack 6G Terahertz Networks [32]	2020				✓	✓	

the received signal back to an intermediate frequency (IF) or directly to baseband, where the digital block enters the game (Sec. III-D). Frequency multipliers can be built utilizing different device technologies:

- **Silicon CMOS and Silicon-Germanium (SiGe) BiCMOS** technologies offer high level of integration with existing electronic systems. However, their maximum transmission power is up to *a few milliwatts per element at frequencies of up to a few hundreds of GHz* [40], [41].
- To increase both the transmission power and the maximum frequency of operation, **III-V semiconductors**, such as Indium Phosphide (InP) and Gallium Arsenide (GaAs), are being utilized to fabricate high-electron mobility transistors (HEMT), heterojunction bipolar transistors (HBT) and Schottky diodes to be utilized in frequency multiplying chains. As of today, transmission power of *hundreds of milliwatts at a few hundreds GHz and up to a few mWs above 1 THz* have been experimentally demonstrated [42], [43].

Independently of the specific fabrication technology, the frequency multiplication and mixing process is *highly non-linear*. This introduces several challenges for THz communications, including high waveform distortion, very high sensitivity to peak to average power ratio (PAPR), and very high phase noise. Moreover, if utilizing transistor-based multipliers as

opposed to diode-based multipliers, high gain is generally achieved at the cost of reduced bandwidth. For example, the bandwidth of the InP HEMT-based frequency-multiplied transceivers is generally less than 10 GHz [42], as opposed to the several tens of GHz of Schottky-diode-based systems [43].

To both increase the transmission power as well as to enable mobile THz networking, *electronic arrays* are being intensively explored. For example, transceiver arrays with 8 parallel channels at 140 GHz have been experimentally demonstrated [44], [45]. Each channel can be utilized to drive independent on-chip antennas in a fully digital MIMO approach or in conjunction with analog antenna arrays to implement hybrid beamforming architectures (Sec. V-B). While on-chip THz antennas are very small thanks to the very small wavelength of THz signals (Sec. III-C), the challenge is to integrate all the electronic components in a thermally stable package [46], [47].

As of 2021, we expect the first commercial THz systems to operate in the lower end of the G-band (from 110 GHz to 300 GHz), and given current technology maturity, these are likely to be based on frequency multiplying chains.

2) *Photonic Approach*: The goal of this approach is to push the limits of photonic techniques utilized in optical wireless systems (OWC) down to the THz band. Currently, there are mostly three approaches to the photonic generation, modulation and detection of THz signals:

- **Quantum Cascade Lasers (QCLs):** These are semiconductor lasers that emit low-energy photons corresponding to far-infrared and THz frequencies [48], [49]. The frequency range of operation of QCLs is generally above 2-3 THz. While output powers of up to a few hundreds of mWs have been demonstrated at cryogenic temperatures, the open challenge is to ensure practical power figures when operating at room temperature [50], [51]. This currently limits their utilization in practical applications.
- **Frequency-difference Generation (DFG):** The fundamental idea of DFG systems is the reciprocal to that of frequency-multiplied electronic systems: a THz carrier signal can be generated by photomixing two optical carrier signals whose wavelength differs by an increment that corresponds to the target THz signal [24], [52]. These systems usually consist of two narrow-band lasers followed by a uni-travelling photodiode (UTC) which acts as a down-converter to THz frequencies [31], [53]. For the time being, these systems have been demonstrated to perform at frequencies of a few hundreds of GHz, with powers of less than 10 mW.
- **Photoconductive antennas (PCAs):** Another technique to downconvert optical signals to the THz band relies on the use of photoconductive antennas [54], [55]. A photoconductive antenna generally consists of a conventional THz metallic antenna printed on top of a photoconductive substrate. When illuminated by an optical signal (normally an optical pulse), photocarriers are excited at the gap of the antenna. A DC bias field is then used to accelerate the carriers along the antenna structure, resulting in the emission of THz photons. The main challenge of this technique relates to the low conversion efficiency and the resulting low emitted power (less than a milliwatt at hundreds of GHz).

The transmission power of photonic THz systems is at least one order of magnitude lower than that of electronic systems and, while the development of photonic THz arrays is an active field of research, these have not been experimentally demonstrated. Nonetheless, the signals generated through frequency down-conversion exhibit higher spectral purity and lower amplitude and phase noise. Moreover, existing large-bandwidth optical modulators can be leveraged to generate high bandwidth THz signals. In light of these, a potential application in which photonic THz systems are likely to be found in the future is in wired fiber optical to wireless THz backhaul applications.

It is relevant to note that there are no photonics-based THz receiver architectures for the time being. Therefore, photonics transmitters are generally used in conjunction with electronic receivers generally based on frequency-multiplying chains in heterodyne configurations as discussed in the previous section.

3) **Plasmonic Approach:** The goal of this approach is to create devices that intrinsically operate at THz frequencies, i.e., without the need to up-convert from the microwave range or down-convert from optics, by leveraging the properties of plasma waves. While some of the first concepts relating to plasmonic generation of THz signals date back over 20 years [56], [57], the discovery and utilization of **new two**

dimensional nanomaterials, such as graphene [58], has opened the door to THz nano-devices able to operate at room temperature. There are several properties of graphene that makes them especially attractive for THz communications. On the one hand, the very high electron mobility at room temperature enables the propagation of **surface plasmon polariton (SPP) waves**, or global oscillation of electrical charges at the interface of graphene and a dielectric material. By leveraging the properties of SPP waves, new devices able to generate [59], [60], radiate [61]–[64] and detect [65], [66] THz signals have been developed [59], [63]. On the other hand, graphene is a highly tunable material, a property that is leveraged to design ultrabroadband modulators in our previous works [67], [68]. This is necessary to ultimately realize the 1 Tbps data-rates envisioned for 6G systems. Moreover, to enhance some of these properties, graphene can be combined with III-V semiconductors or with other 2D materials, such as hexagonal boron nitride (hBN) or molybdenum disulfide (MoS₂).

Plasmonic THz devices *naturally operate at frequencies above hundreds of GHz and few THz with bandwidths in excess of 10% of their carrier frequency*. In addition, they are very small, i.e., in the order of hundreds of nanometers or a few micrometers. Note that this is much smaller than the THz wavelength, because of the plasmonic confinement factor. The very small size plays a dual role in THz communication systems. On the one hand, *even if energy efficient, the total radiated power by a single device is very low, in the orders of a few microwatts at most*. On the other hand, their very small size allows their adoption the nanoscale applications discussed in the introduction [11], [69], but also their integration in very dense compact arrays [70], [71]. Nevertheless, compared to the electronic and photonic approaches, which have been refined over decades of research, the plasmonic approach is still in its early stages. In our vision, the plasmonic approach has the potential to enable compact, energy-efficient and intelligent distributed THz systems.

Other non-conventional devices for THz communications include **phase-change materials**, including vanadium dioxide (VO₂) and liquid crystals [72], [73]. Specifically, phase-change materials can be utilized as tunable elements at the transmitter and the receiver to support high-speed modulation (in addition to phase controllers in antenna systems, discussed in Sec. III-C). Furthermore, the application of **superconductors** like Bi₂Sr₂CaCu₂O_{8+δ} (BSCCO) also enable tunable plasmonic THz sources [74].

Overall, the plasmonic approach to THz communications is a less mature and conservative path than the electronic and photonic approaches, with *high risk but also very high rewards*, arising from true THz operation, ultrabroadband bandwidths, and support for high reconfigurability and tunability.

As a summary of this section, the block diagrams for the three most common analog front-end architectures for THz wireless systems is shown in Fig. 7.

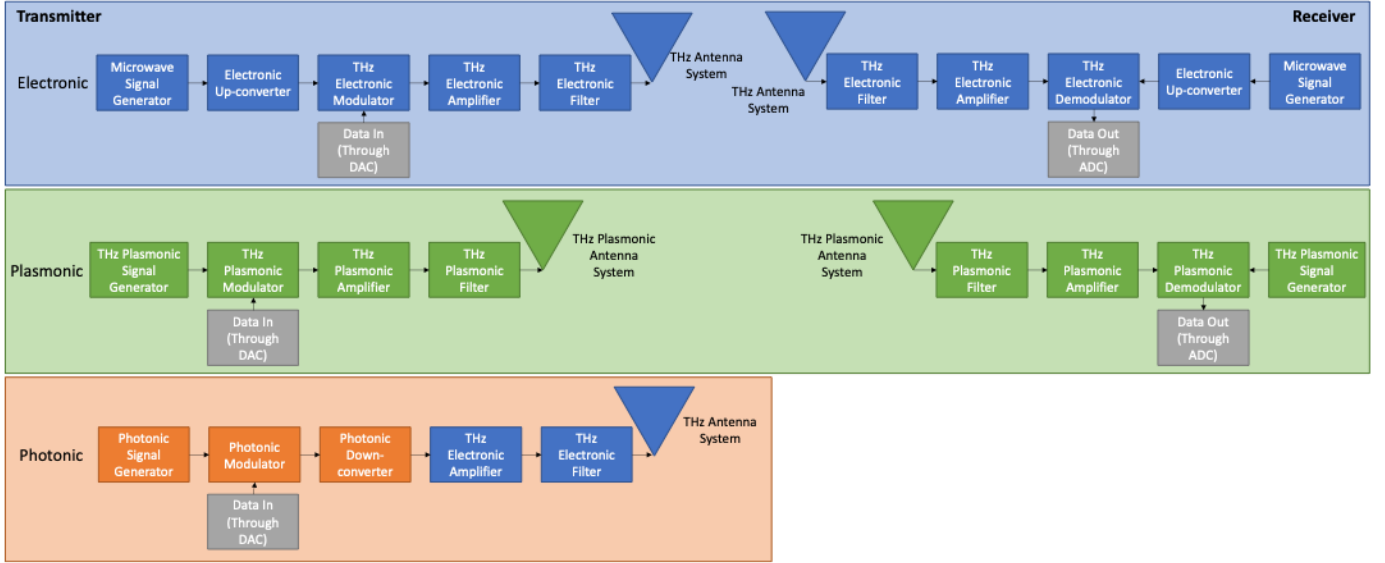


Fig. 7. Block diagram for the three most common transceiver architectures based on: (top) An electronic frequency-upconverting system; (middle) A plasmonic direct THz heterodyne system; and (bottom) A photonic frequency-downconverting transmitting system (note that there are no photonic-based THz receivers).

C. Intelligent Antenna Systems in Transmission, Reception and Reflection

Antennas are needed to convert the on-chip signals into wirelessly propagating waves. In contrast to analog front-ends, where there are clear divisions between electronic, photonic and plasmonic systems, antenna systems are much more flexible. For example, conventional antennas are generally used in conjunction with electronic and photonic front-ends, whereas plasmonic antennas are needed for plasmonic front-ends. Similarly, optical lenses can be used in conjunction with any type of antenna. We explain these in detail next.

The very small wavelength of THz signals enables the development of very small conventional THz antennas. For example, a 150 μm long printed dipole or patch antenna resonates at approximately 1 THz and exhibits a quasi-omnidirectional radiation pattern. Moreover, if adopting graphene and/or other plasmonic materials, the plasmonic confinement factor can be leveraged to design THz antennas which are even smaller. For example, a graphene-based plasmonic nano-patch antenna designed in our previous work to resonate at the same 1 THz would be just 1 μm long and 10 nm wide, i.e., two orders of magnitude smaller than the metallic antenna [63]. The very small size of these antennas is what enables their application in wireless networks on chip or even wearable and implantable devices (Fig. 2).

Nevertheless, this very small size also results in a very small antenna effective area and, correspondingly, very high spreading losses (Sec. IV-C). Increasing the effective area of THz antennas automatically leads to antennas that no longer radiate omnidirectionally, but are highly directional. For the time being, there are mostly two main types of directional antenna systems:

- **Fixed directional antennas:** These include horn antennas, with typical directivity gains in the order of 20-25 dBi (or gain in dB over an isotropic antenna);

Cassegrain dish reflector antennas, with directivity gains around 40-55 dBi; as well as more sophisticated designs such as multi-reflector antennas [75], with gains of up to 30-35 dBi. Many of these are commercially available [76], [77]. Other less conventional fixed directional radiating structures include leaky wave antennas, whose direction of radiation depends on the frequency of excitation, which opens the door to new ways of spatial and frequency multiplexing [78], [79].

- **Beamforming antenna arrays:** These can be either fixed or dynamic, and can be built either with traditional metals or by leveraging new nanomaterials. For example, on the one hand, metallic antenna arrays utilized in conjunction with electronic front-ends have been demonstrated at frequencies under 300 GHz [44], [80], [81] with up to 16 controllable elements. On the other hand, in conjunction with plasmonic front-ends, very large graphene-based plasmonic antenna arrays with up to 1,024 elements have been proposed [70], [71], [82]. The latter are at the basis of ultra-massive MIMO systems, as we discuss in Sec. V-B.

In both cases, **dielectric lenses** can be utilized to further increase the gain and dynamic capabilities of directional THz antenna systems. For example, a silicon lens printed on top of an on-chip quasi-omnidirectional antenna can provide up to 30 dBi of gain [83]. Similarly, commercially-available lens-integrated horn antennas can achieve gains in the range of 40-55 dBi, in a more compact form factor than that of dish reflector antennas. Moreover, lenses can also be utilized in conjunction with arrays. For example, in [84], an array of lenses deposited on top of an array of on-chip antennas is experimentally demonstrated. Alternatively, a single large footprint lens can be utilized on top of a beamforming antenna array, for which the beamforming weights would need to be designed accounting for the lens-corrected propagation path.

In addition to fixed lenses, **programmable lenses based on**

metamaterials can also be utilized at THz frequencies [85]–[88]. Metamaterials and metasurfaces are engineered structures (in 3D and 2D, respectively) designed to exhibit EM properties not commonly found in nature. Metamaterials are composed by well-defined arrangements of meta-atoms, which are generally metallic structures. By definition, the size of the meta-atoms is much smaller than the wavelength corresponding to the frequency at which the structure is designed to operate. This is a key difference from traditional metallic antenna arrays, with which many times metasurfaces are compared. Perhaps more importantly, antennas are transducers that convert electrical energy into EM energy and vice-versa, as opposed to metamaterials, in which the input and the output are EM signals. Besides lensing, transmit metasurfaces can also be utilized to perform communication functions of the chip, such as modulation [89], polarization manipulation [90], and holographic projections [91].

Besides transmission and reception, **antenna arrays and metasurfaces can also be utilized in reflection and, thus, as enablers of intelligent reflecting intelligent surfaces (RISs)**. RISs are a key technology to enable intelligent propagation environments in 6G systems [3], [92]. While RISs at lower frequencies are mostly used to increase the achievable data-rates, at THz frequencies RISs are a critical infrastructure to overcome the need for line-of-sight (LoS) propagation (Sec. IV-C). RISs can precisely control the reflection of incoming THz signals in specular and non-specular paths, while changing the polarization or adding an additional level of modulation if needed. Fixed THz reflecting surfaces based on reflecting antenna arrays or reflect-arrays as well as metasurfaces have been experimentally demonstrated for years [93]–[95]. The challenge is to make them reconfigurable. In contrast to lower frequency bands, where tunable capacitors or diodes can be utilized to change the reflection coefficient of individual antenna elements or the behavior of individual meta-atoms, at THz frequencies new tunable elements are needed. The tunability of graphene can be leverage for this purpose. For example, in [96], a graphene-based plasmonic reflect-array was proposed. However, graphene is not a good reflecting material compared to traditional metals. To overcome this channel, we have proposed hybrid graphene-metal structures recently [97], [98], which combine the tunability of graphene with the reflectivity of gold. On the metamaterial front, we have proposed hypersurfaces [99], [100] to enable reconfigurable metasurfaces that can achieve different functionalities across the spectrum, including the THz band [101].

In addition to the spatial properties of these radiating structures (e.g., number of beams, beamwidth, etc.), **the antenna bandwidth plays a key role**. With only few exceptions (such as in impulse-radio ultra-wide-band systems), antennas utilized in commercial communication systems are generally narrowband, i.e., the bandwidth of their frequency response is much less than 10% of the carrier signal. Antenna systems effectively acts as filters and, thus, can introduce distortion to the transmitted waveforms if these exceed the antenna bandwidth. Such dispersive effect, many times attributed to the channel, is in fact an antenna factor and, thus, the design of ultrabroadband antennas becomes critical. Even if the

radiating elements themselves exhibit large bandwidth, the other building blocks of antenna or meta-atom arrays need to be large bandwidth. For example, in antenna arrays, broadband phase controllers or, reciprocally, time-delay lines are needed to prevent beam squint [102].

Finally, additional opportunities for THz antenna systems include the development of structures that can enable the **engineering of wavefronts** different than the traditional Gaussian beams. For example, self-healing Bessel beams [103] or bending Airy beams [104] can provide additional capabilities to intelligent THz propagation environments. Moreover, on top of the wavefronts, orbital angular momentum (OAM) can be defined [105], [106]. Often compared to MIMO, OAM creates intrinsically orthogonal parallel spatial channels, without the need of sophisticated digital signal processing and working even (or especially) in LoS propagation conditions. Such OAM modes can be utilized to increase the capacity of THz systems without increasing the system bandwidth.

D. The Digital Bottleneck

Enabling 1 Tbps links requires not only the development of analog front-ends and antenna systems that can operate at higher frequencies and with larger bandwidths, but also the development of a digital signal processing back-end that can generate at the transmitter and process at the receiver the information at such very high data. For the time being, all DSP solutions rely on electronic devices, mostly because of all the commercial computing cores are electronic systems. While there are early concepts of fully optical processors [107], [108] and even plasmonic processors [109], [110], these are not likely to become a reality within 6G systems. Therefore, we focus on electronic DSP systems.

Common with the fastest wired communication systems over optical fiber, the main bottleneck for ultra-broadband digital THz communications is posed by **the performance of DACs and ADCs**. More specifically,

- At the transmitter, state-of-the-art DACs able to sample at frequencies in excess of 100 Giga-samples-per-second (GSaps) have been experimentally demonstrated. For example, in [111], two 128 GSaps DACs are multiplexed to effectively sample at 256 GSaps. This translates to a signal bandwidth of at most 128 GHz (and practically much less if meaningful oversampling gain is needed). However, this comes at the cost of low sampling resolution (only 2-bits) very high power requirements, thermal dissipation and large footprint.
- The situation is not that different at the receiver. Generally, higher sampling frequency and higher resolution ADCs have been developed, many times driven by the scientific sensing community performing remote sensing experiments at THz frequencies. Time-interleaving is also the solution commonly adopted to increase the sampling frequency of ADCs [112]. Again, this comes at the cost of strict power, thermal and space requirements.

Other time- and frequency-multiplexed systems that can operate at 256 GSaps with 8 bits resolution are at the basis of

commercial-grade equipment utilized in experimental testbeds (discussed in Sec. VII).

To overcome the digital bottleneck, different strategies are being explored. On the one hand, the analog system bandwidth is divided into narrower channels in our previous work [113], to be individually digitally processed and analogically frequency-multiplexed at the transmitter and demultiplexed at the receiver [114]. Alternatively, instead of sacrificing the sampling frequency, we have utilized a large number of very low resolution ADCs to reliably demodulated sophisticated waveforms despite heavy quantization in large arrayed systems [102]. Clearly, the development of faster DACs, ADCs and digital signal processing (DSP) algorithms will benefit not only THz communication systems, but any high speed wired or wireless communication and sensing technology.

E. Fabrication and Integration Challenges

In addition to the individual challenges related to analog front-ends, antenna systems and digital back-ends previously highlighted in each section, there are challenges that affect all of the building blocks. These include

- **Heterogeneous integration and fabrication.** Different of the aforementioned building hardware blocks rely on different material and device technologies, ranging from silicon CMOS for high-density integration, to III-V semiconductors for power or graphene for tunability and bandwidth. Heterogeneous integration refers to not only the combination of different components based on different materials, but also co-design of the different blocks, exploration of impact of different blocks on each other, and definition of scalable and cost-effective fabrication processes. In our vision, to achieve optimal trade-offs among multiple metrics including frequency, bandwidth, power, cost, and energy-efficiency, the joint consideration of diverse materials and fabrication, containing photonics-based, electronics-based, nanomaterials-and-plasmonics-based approaches, is a promising research direction for practical THz communication systems.
- **Terahertz devices for extreme environments:** As mentioned in the introduction, the applications of THz communication networks range from nanoscale intra-body or wearable networks to inter-satellite links in space. Different environments impose very different operation conditions. Inside the body, the use bio-compatible layers to *disguise* non-biological structures from the immune system are needed. Similarly, the THz devices used in space bear noticeable differences from the ones in the terrestrial scenarios. It is relevant to note, however, that there have been satellites orbiting the Earth with THz systems (mostly power detectors) for over a decade [25], [115]. These are based on III-V Schottky diode technology. Space-proofing other of the needed technologies for extreme space applications is a necessary step to enable applications such as TeraSpace.

IV. PHY LAYER: CHANNEL MODELING AND CHARACTERIZATION

Besides practical THz devices, the realization of THz communication requires a thorough investigation of the THz channels as well. Unlike the low-frequency electromagnetic waves, the distinctive attributes of the THz spectrum have motivated novel techniques to model and measure the THz channels. In particular, the high propagation loss, the frequency-dependent molecular absorption, among others, bring challenges to the traditional channel modeling. In this section, we explore channel measurement methods, study and assess channel modeling schemes, analyze channels and corresponding propagation characteristics, and present open research challenges.

A. Channel Measurements

The first studies of THz wave propagation were largely theoretical and mostly driven by the atmospheric sensing community. Radiative transfer theory is found at the basis of closed-form analytical models for THz wave-matter interactions, which play a critical role in the propagation of THz signals. Similarly, the first complete channel models for the THz band, including our own [116], [117], are derived through the combination of physics, electromagnetics and communication theory.

Among other techniques including EM wave theory and full-wave simulation, channel measurement is essential to characterize the spectrum features and develop channel models. Recently, with the progressive narrowing of the THz technology gap, experimental measurement campaigns in the lower THz band have been conducted [118]–[121]. Such experimental measurements play a dual role: on the one hand, they can be used to validate the analytical physics-driven models. On the other hand, empirical data-driven models, much simpler than their physical counter-parts, can be developed. The latter are generally preferred by standardization bodies, such as the 3GPP.

Although multiple measurement approaches have been practically utilized for a long time, THz channel measurement systems need to measure wideband characteristics, support long-distance sounding given the high path loss, and consume reasonable time by scanning the spatial domain even with high-directivity antennas. We describe the three main THz channel sounding techniques next (Fig. 8).

1) *Frequency-domain Vector-Network-Analyzer-based Method:* A Vector Network Analyzer (VNA) is commonly utilized to measure the frequency response of a linear system one frequency at a time. VNAs are commonly used to characterize discrete electrical/RF components, and can be utilized to measure the wireless channel by connecting antennas at the transmitting and receiving ports. The VNA suffers from low output power, high noise, limited distance, as well as long measurement times. The first two issues, i.e., low output power and high noise, can be mitigated by exploiting external power and low-noise amplifiers. The distance can be extended via optical fiber and directional transmissions. However, the long measurement times still hinder the application of VNA in dynamic THz channels [122].

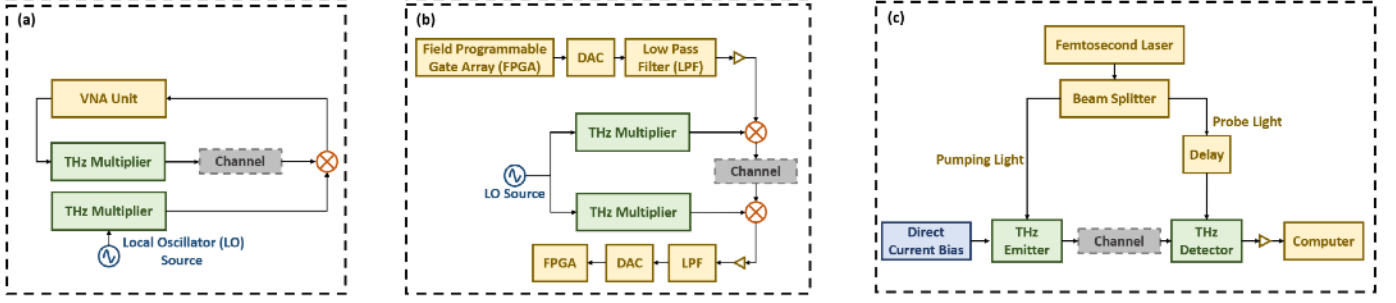


Fig. 8. Channel measurement techniques. (a) VNA-based method, (b) sliding correlation method, and (c) direct pulse method.

Based on this VNA method, we have built a 140 GHz channel measurement system with Huawei, enabling the end-to-end measurement solutions for an indoor meeting room [123]. Using this system, the channel parameters, as well as the temporal and spatial distributions of multipath scenarios, are investigated by Shanghai Jiao Tong University (SJTU) [123]. Furthermore, we have improved this system to support channel measurements at 220 GHz for LoS and Non-Line-of-Sight (NLoS) paths in an office and a hallway [124]. Similarly, the University of Southern California (USC) has utilized the VNA based method to create a channel measurement system for urban scenarios at approximately 140 GHz [125]. To expand the transmission distance from 8–10m to 100 m was realized through the above mentioned optical fibers in [125]. Further, the measurements up to 220 GHz band is realized in [126]. The VNA-based measurements at 300 GHz have been conducted at Georgia Tech for a desktop [127], a computer motherboard [128], and a data center [129].

2) Time-domain Sliding Correlation Method: Another channel measurement approach is based on the transmission of a signal whose autocorrelation is a Dirac delta function, where the channel can be considered time-invariant. Such a correlation-based technique allows the exploitation of high transmit power with a low PAPR. The advantage of this method is that real-time measurements can be realized. However, there exist two main drawbacks with this method. On the one hand, the power spectral density tends to be distributed unevenly. On the other hand, ultra-high sampling rate DACs/ADCs are needed. The second problem can be addressed due to the fact that the sliding correlation method expands the measurement duration and accordingly increases the SNR because different chip rates can be utilized for the correlation process between transmitter and receiver [130].

This method is used in the establishment of a real-time measurement platform operating at 140 GHz at the New York University [131]. This platform is utilized for reflection and scattering propagation characteristics in [132], large-scale fading and multipath characteristics of indoor channels in [133], as well as analyses of receive powers and interference for satellite measurements in [134]. Another correlation based measurement system is developed for 300 GHz at the Technische Universität Braunschweig in [135]. They cooperated with Beijing Jiao Tong University (BJTU) and conducted measurements of 60–300GHz channels utilized for China high-speed rail in [136], [137] with the train-to-infrastructure inside-

station channels [138] and intra-wagon channels [139]. The same setup is utilized for channel measurements of single-lane and multi-lane vehicle-to-vehicle communications in [140] and attenuation by the window and fuselage of a Boeing 737 aircraft [141].

3) Direct Pulse Method: In parallel to the above two approaches, the direct pulse method, also known as THz time-domain spectroscopy (THz-TDS), is the most straightforward, which trains very narrow pulses in the time domain with a period larger than the maximum excess delay (i.e., the relative delay between the first-arriving component and the multipath component whose energy falls below a certain threshold from the strongest one). Using this measurement method, the channel impulse response can be easily obtained from the observation of the received signals. This can be realized by considering the amplitude of the channel impulse response as well as the delay between the transmission time and sampling time. This method is suitable for the THz waves with ultra-broad bandwidth [142], while incurring low power, large equipment size, short distance, as well as the range of applications limited to the measurements of reflection, scattering, and diffraction properties induced by the narrow beams.

We have used the THz-TDS method to measure the interference of THz channels at 300 GHz and analyzed stochastically [143]. Measurements have been conducted to study reflection coefficients of building materials at 100–1000 GHz [144] and those of stratified building materials [145] by teams from Brown University and the Technische Universität Braunschweig. This method has also been applied to measure diffusion coefficients of rough surfaces at 200–400 GHz [146].

B. Channel Modeling Methodologies

On the basis of THz channel measurements, channel characterization is needed to support subsequent research on the PHY layer and above, whereas existing channel models for lower frequencies are not directly applicable to the THz band, thus motivating different channel modeling methodologies. Current channel characterization can be performed deterministically, stochastically, or in a hybrid manner combining both synergistically.

1) Deterministic Channel Modeling: Starting from the EM wave theory [147], deterministic channel models provide an accurate description of wave propagation. Numerical results

generally conform to the measurements, while the complete geometric information of the wireless environment, attributes of materials, and exact locations of the transceivers are indispensable. Specifically, we survey two commonly utilized schemes in the context of THz communications.

- **Ray-tracing (RT)** is a promising choice in modeling site-specific wireless environments and keeps reasonable computational complexity in very large systems. In particular, a fixed transmitter generates signals that encounter different objects with various surface conditions along propagation. Upon reception, the reflected, diffracted, or scattered arrival rays beside the LoS one are captured. By analyzing the wavefronts of each ray as simple particles, the RT explores characteristics of these electromagnetic waves. In practice, RT can be realized over several methods. A typical method is representing the transmitter as the root node and recursively seeking branches (i.e., objects in the wireless environment that can be connected to this root node in a LoS manner), until the receiver branch is reached. In this way, the RT develops a visibility tree of deducing paths through the backtracking methods. The other approach is a strategy called ray launching, which radiates rays in a predetermined grid of directions and explores the trajectory [148].

Since THz signals have stronger corpuscular properties compared to low-frequency bands, geometric optics can be used to accurately simulate the loss in reflection, diffraction, and scattering [26]. Recently, in consideration of the suitability of the RT for THz waves, tailored RT modeling for the THz band has been conducted. For example, the RT method is invoked at 300 GHz in an indoor scenario [149], which is calibrated by channel measurements to improve the accuracy. In addition, we exploit the RT method to generic multipath THz channel models that are applicable to the entire THz spectrum [117]. Besides, by accounting for the elevation plane apart from the conventionally considered azimuth plane, we have successfully applied the RT method to build 3D end-to-end THz channel models [150], [151]. We also discuss several available THz channel simulation platforms that build on RT theory are available as well (discussed in Sec. VII).

- In parallel to the RT, the **finite-difference time-domain (FDTD) or Yee's method** [152] numerically derives the channel model from Maxwell's equations. Specifically, to accelerate the computation, the whole space is divided into grids that are separately explored. Then, both the electric and magnetic fields are analyzed and iteratively updated in the temporal and spatial domains. Considering the rigorous theoretical computation, the FDTD can model small and complex scatterers and rough surfaces with high accuracy. However, the high accuracy is achieved at the expense of a substantial computational burden in both memory and time in attaining all geometrical features along propagation.

2) *Statistical Channel Modeling*: Based on large datasets obtained from empirical channel measurements, statistical

channel modeling (SCM) method has an advantage of low computational complexity compared to the aforementioned deterministic modeling alternative. Since the THz channel is deemed spatially sparse with resolvable multipath components, tailored models are necessary in lieu of narrowband models, in which Rayleigh or Rician fading is commonly assumed.

Some SCM models characterize the temporal and spatial channel characteristics with fitted distributions, such as directions of departure/arrival (DoD/DoA), time of arrival (ToA), as well as complex amplitudes. The Saleh-Valenzuela (S-V) model with the tapped delay line [153] can be used to describe clusters of multipath components. An example of such a model at 300 GHz can be found in [118]. By contrast, some SCM models describe the impulse response of channel and antenna characteristics mathematically without the explicit consideration of propagation. On the one hand, the simple assumption of independent and identically distributed (i.i.d.) Rayleigh fading channel model is widely studied. Nevertheless, the i.i.d. model is not suitable for the THz band due to the high sparsity. On the other hand, the Kronecker model considering correlation between sub-channels is conventionally utilized as well. However, in UM-MIMO channels, the Kronecker model can lead to high bias [26]. To address those problems, virtual channel representation (VCR) is proposed to explore the beam space when sampling rays for UM-MIMO systems [154], which however only focuses on uniform linear arrays. Furthermore, our previous work illustrates that the integration of the Kronecker and VCR models, namely, the Weichselberger model, is valid for various UM-MIMO scenarios [26].

3) *Hybrid Channel Modeling*: As described in Secs. IV-B1 and IV-B2, deterministic channel modeling achieves high accuracy at the expense of low time and resource efficiency. By contrast, statistical channel modeling works with a low computational burden while sacrificing accuracy. Thus, by strategically fusing two or more approaches, the development of *hybrid methods* is attractive and promising to resolve complex THz channel models under low latency.

For instance, a combination of RT and FDTD methods can realize accurate modeling in a time-efficient manner [155]. Specifically, the FDTD with high accuracy assists the modeling in the region close to scatterers, while the RT is in charge of modeling the rest of the wireless channel. This hybrid method has been utilized in [156] for indoor channel modeling. Compared to the individual methods, this hybrid scheme is preferred in THz communications due to its high time efficiency and accuracy.

Furthermore, the hybrid approach can provide even higher computation efficiency owing to the stochastic component. Sufficient channel information can also be captured for ease of higher accuracy thanks to the deterministic part. With the DoA following a Gaussian mixture model (GMM), this hybrid modeling has been implemented at 0.3 THz for an indoor scenario [157]. By generating angles of arrival (AoAs) with Von Mises distributions, we have established a semi-deterministic THz channel model in [119]. Moreover, a generic 3D THz channel model under non-stationarity is proposed, which jointly considers space, time, and frequency domains [158].

C. Channel and Propagation Characteristics

In addition to the aforementioned modeling techniques, a comprehensive understanding of fundamental spectral and spatial characteristics is critical. We hereby summarize them in Table II and elaborate as follows.

- 1) *Spreading Loss*: The Friis' law with frequency-independent antenna gains suggests that when the antenna apertures at both link ends decrease, the spreading loss increases quadratically. However, fixed-aperture antennas with frequency-dependent gains will lead to a quadratic drop of the loss.
- 2) *Atmospheric Loss*: The atmospheric loss or molecular absorption loss is caused by the partial conversion of THz wave energy into a rotational transition form for polar gas molecules in the propagation medium. Such molecules are usually composed of water vapor and oxygen molecules. As a result, the power of the THz signal is attenuated, while the noise is amplified [159]. Moreover, the absorption peaks create spectral windows in the THz band, which are distance-varying [26]. For example, as shown in Fig. 9, two windows at 0.38–0.4 and 0.62–0.72 THz with a 30 m transmission distance merge into one at a distance of 1 m. Compared with other spectrum bands used for wireless communications, the atmospheric loss is relatively small for both mm-wave (caused by oxygen molecules) and OWC communications (owing to water vapor and carbon dioxide molecules), while negligible in microwave communications. Such a noticeable atmospheric loss in THz band requires physical layer designs with distance adaptivity and multi-wideband capability [160].
- 3) *Temporal Broadening*: Besides spectral windows, the frequency-selectivity of THz communications incurs broadening in the temporal domain. By defining the *broadening factor* as the quotient of the durations for the received and transmitted pulses, the minimal interval between consecutive transmissions without inter-symbol interference can be quantified. The value of this factor increases with growing signal bandwidth, operating frequency, and transmission distance [117], hence limiting the transmission rate.
- 4) *Diffuse Scattering and Specular Reflection*: The comparable scales of wavelength in the THz band and the surface roughness of common objects incur severe diffuse scattering on rough surfaces, where scattered rays are radiated to various directions.
The loss stemmed from specular reflection is a function of the electrical thickness of the surface, which is a frequency-dependent parameter. With respect to all multi-paths, the received power from specular reflection is generally dominant as compared to that of diffuse scattering. Moreover, as the frequency increases, the surface roughness parameter that determines the scattered power declines, while the surface correlation parameter controlling the scattered beam width increases. In the sequel, the rays at very high frequencies travel in all directions with uniform power after encountering severely rough surfaces.
- 5) *Diffraction, Shadowing, and LoS Probability*: Due to the sharp shadows of various objects, such as walls and people, the efficiency of diffraction decreases with increased frequency. Hence, in practice, diffraction can be neglected so long as the receiver is in a very closed region approaching the incident shadow boundary. As a consequence, as the frequency increases, shadow fading variance becomes more significant. Moreover, the area within the first Fresnel zone that is especially vulnerable to shadowing objects reduces with the square root of the wavelength. In addition, generally, the frequency does not impact the LoS probability. However, owing to the skin effect in lossy media, transmission power decreases near uniformly with increasing frequency.
- 6) *Coherence Bandwidth*: Within the range of coherence bandwidth that is inversely proportional to the delay spread, the signal can be transmitted without undergoing the frequency-selective fading. In the THz band, the larger propagation distance induces the narrower coherence bandwidth [117], and by altering the distances as 2 m, to 3 m, 4 m, 5 m, and 6 m, the average coherence bandwidths are 3.42 GHz, to 2.56 GHz, 2.17 GHz, 1.75 GHz, and 1.47 GHz, respectively. In addition, our beamforming design elongates the THz signals for farther while slenderer coverage, resulting in a reduction for MPC and thereby a wider coherence bandwidth [150].
- 7) *Stationarity Time and Stationarity Bandwidth*: Stationarity time and bandwidth are defined as the period and the spectrum range that emerges wide-sense stationary channels in time-varying THz communications. Compared with the coherence region [161], the stationary region in THz vehicle-to-everything (V2X) communications is much larger, since the stationarity region depends on the statistical channel parameters, while the coherence region is determined by the exact values for these parameters. Furthermore, the shorter stationarity distances suggest the heavier non-stationarity in THz V2X channels. Experiments demonstrate the approximate 0.37 m stationarity distance when the receiver moves with a velocity of 15 m/s, revealing the small variation of the approximate wide-sense stationary environment within 0.37 m.
- 8) *3D Angular Spread*: As a key to spatially characterizing the 3D channels, especially those equipped with UM-MIMO, the angular spreads need to be studied in the elevation plane as well as the azimuth plane. According to the trials in our previous work, the beamforming and the relative locations between the transmitter and receiver remarkably affect the angular spreads [150].
- 9) *Spatial Degree of Freedom*: The spatial degree of freedom depends on the array area, array geometry, and angular spread. This parameter measures the largest spatial multiplexing gain that can be supported by a UM-MIMO system [162]. Therefore, the large angular spread in a rich scattering environment leads to a sizable spatial degree of freedom.

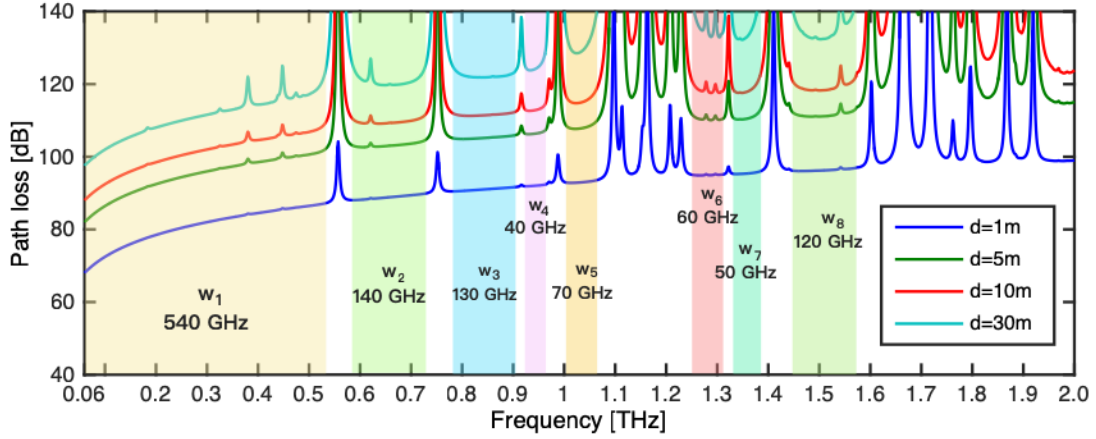


Fig. 9. Path loss in the THz band. Eight spectral windows are identified and their bandwidths range from 40 GHz up to 540 GHz.

- 10) *Weather Influences*: The aerial particulates, including rain, fog, haze, smog, etc., further increase the THz propagation loss. This property can be characterized via the Mie scattering theory when airborne particles are in the comparable size of the THz wavelength. Otherwise, with smaller airborne particle sizes, the Rayleigh model is used to approximate the Mie scattering model. In addition, when the sky is not clear, considerable attenuation occurs on the infra-red or OWC rays whose wavelengths are smaller. However, better robustness against weather influences emerges at the THz band, since the THz signals are less susceptible when traveling through small airborne particulates.
- 11) *Scintillation Effects*: The presence of thermal turbulence near the ground incurs the spatial and temporal inhomogeneities of temperature and pressure across time and space in the air. As a result, scintillation can arise. In particular, the various refractive indices for the wavefront of a beam and unevenly distributed deflection and interference lead to the distortion of the flat phase front of the beam. Owing to this effect, a twinkling speckle pattern, which contains severe temporal variations on intensity, occurs in the beam cross-section at the receiver. In comparison, the THz communications are immune to the effects of scintillation, while these effects confine the largest distance of OWC communications.

D. Link Budget Analysis

To support the realistic commercialization applications, the effectiveness and reliability of THz communication systems should be verified. To this end, practical link budget indicators need to be thoroughly evaluated in the THz band, including frequency, desired data rate noise figure, etc. Two fundamental knowledge are required to calculate the THz link budget. In particular, on one hand, theoretical THz propagation and channel characteristics provide prerequisite calculus terms for link budget, which are discussed in Sec. IV-C. On the other hand, numerous practical measurement campaigns elaborated in Sec. IV-A can be a good guideline for the link budget analysis. For example, we list the THz link budget for an

indoor scenario in Table III. More specifically, to achieve 1 Tbps downlink, 1,024 Tx antennas, 64 Rx antennas, and 4 data streams are deployed, and the link distance is 1 meter. Note that these parameters are adjusted according to the simulation with the noise figure computed by following the scheme in [163]. If the desired data rates are 100 Gbps at the uplink and 200 Gbps at the downlink, a transmission distance longer than 10 m can be achieved.

We conduct another analysis investigates the link budget parameters for AR/VR-fronthauling as well as backhauling in [164], to provide a quantitatively perspective on such systems at 287.28 GHz. Specifically, for AR/VR over 10 m, the achievable rate reaches 20 Gbps with 10 GHz bandwidth and 10 dBm transmit power. By contrast, the rate for backhauling achieves 200 Gbps, when the bandwidth and transmit power increase to 100 GHz and 20 dBm, respectively. The distance in this scenario can extend up to 2 km if 55 dBi antenna gain is available.

E. Open Problems

- **Efficient THz Channel Measurement Systems.** Most of the existing measurement methods are adapted from systems designed for low-frequency bands, i.e., mm-wave. However, as we mentioned in Sec. IV-C, the special properties of THz waves motivate more advanced and flexible systems to handle significant path loss, ultra-large bandwidth with high frequency, as well as short coherence time. Based on such systems, extensive channel measurement campaigns should be conducted for various scenarios, such as unmanned aerial vehicles assisted wireless communications, virtual/augmented/mixed/extended reality (VR/AR/MR/XR), nano-communications, etc., for ease of the practical implementations of these THz applications.
- **Accurate and Flexible THz Channel Models.** The discussions in Sec. IV-B1 reveal the shortage of the commonly used deterministic and stochastic channel models for THz communications. These issues motivate the integration of deterministic and statistical modeling approaches to reach both high efficiency and accuracy un-

TABLE II
THz CHANNEL FEATURES AND IMPACT ON 6G WIRELESS COMMUNICATION AND NETWORKING.

Parameter	Dependence on frequency	Impact on 6G THz systems	THz vs. Microwave and OWC
Spreading Loss	Quadratic increase with decreasing area and constant gains; Quadratic decrease with constant area and frequency-dependent gains	Distance limitation	Higher than microwave, lower than OWC
Atmospheric Loss	Frequency-dependent path loss peaks appear	Frequency-dependent spectral windows with varying bandwidth	No clear effect at microwave frequencies, oxygen molecules at millimeter wave, water and oxygen molecules at THz, water and carbon dioxide molecules at OWC
Temporal Broadening	Increase with bandwidth, frequency, and distance	Limited minimal spacing between consecutive pulses and data rate	Stronger than microwave, weaker than OWC
Diffuse Scattering and Specular Reflection	Diffuse scattering increases with frequency. Specular reflection loss is frequency-dependent	Limited multi-path and high sparsity	Stronger than microwave, weaker than OWC
Diffraction, Shadowing and Line-of-Sight Probability	Negligible diffraction. Shadowing and penetration losses increase with frequency. Frequency-independent LoS probability	Limited multi-path, high sparsity and dense spatial reuse	Stronger than microwave, weaker than OWC
Coherence Bandwidth	Decrease with longer distances and constant numbers of MPCs; increase with constant distances and fewer numbers of MPCs	Limited data rate without the frequency-selective fading	Broader than microwave, narrower than OWC
Stationarity Time and Stationarity Bandwidth	Decrease with frequency	Constraint in mobile system design	Smaller than microwave, larger than OWC
3D Angular Spread	Decrease with frequency	Constraint in beamforming and beam tracking design	Smaller than microwave, larger than OWC
Spatial Degree of Freedom	Decrease with frequency	Constraint in beamforming and beam tracking design	Smaller than microwave, larger than OWC
Weather Influences	Frequency-dependent airborne particulates scattering	Potential constraint in THz outdoor communications with heavy rain attenuation	Smaller than microwave, larger than OWC
Scintillation Effects	Increase with frequency	Constraint in THz space communications	No clear effects at microwave, THz is less susceptible than OWC

TABLE III
THz LINK BUDGET FOR DIFFERENT SCENARIOS.

Parameter	Uplink	Downlink
Frequency	300 GHz	
Bandwidth	30 GHz	
Target achievable rate	1 Tbps	
Tx beamforming gain	18.1 dBi	30.1 dBi
Rx beamforming gain	30.1 dBi	18.1 dBi
Transmit power	5 dBm	13 dBm
Link distance	1 to 100 m	
Rx noise figure	10 dB	
Number of Tx antennas	64	1024
Number of Rx antennas	1024	64
Antenna gain	5 dBi	
Achievable Rate	1171 down to 12.8 Gbps	1490 down to 50.1 Gbps

der multi-paths. However, the smooth transition between different modeling schemes, the requirement of substantial measurement campaigns, and the complex parameter extraction is still a challenge. The design for accurate and flexible hybrid models is thereby limited. Moreover, considering the promising prospect of THz UM-MIMO systems with high spectrum and power efficiency, the high-performance THz UM-MIMO channel modeling is significant for next-generation wireless communications. However, the large-scale antenna arrays exploited by UM-MIMO systems lead to multiple issues that need

to be innovatively addressed for modeling, including the complex analysis and mutual coupling effect.

- **Outdoor and Mobile Channel Measurements and Models.** Recently, some THz channel measurements and modeling solutions have been for several outdoor and mobile scenarios, including vehicular networks [140], terrestrial and satellite spectrum sharing systems [134], airplane-satellite [165], as well as inter-satellite links [166]. This suggests that the outdoor and mobile THz channels have drawn remarkable research attention, while further investigation of non-stationary and outdoor scenarios still remain open problems.
- **AI-enabled Channel Modeling.** Thanks to the sustaining advancement of AI techniques, AI-based wireless communication has immense potential to address complicated problems. Hence, taking into account the special THz properties together with the requirements of accurate multi-path channel measurement analysis and modeling, AI techniques are preferred by the complex THz systems.

V. PHY LAYER FUNCTIONALITIES

In light of the ongoing THz hardware and channel developments, efficient PHY layer technologies are needed to meet the constantly increasing system and network requirements. Till date, the hardware implementations are still rare, and only a few of the works discussed in this section have been in fact experimentally validated. Promisingly, diverse theoretical

designs have been proposed, which are potential to realize efficient communication in the THz band. In this section, we focus on innovative technologies at the physical layer.

A. Modulation and Coding Schemes

Modulation and coding are the primary elements for reliable wireless communication designs. Considering unique device and channel properties in the THz band, classic modulation and coding schemes need to be revisited while new ideas to be developed. When we started exploring the physical layer of THz communications in 2010 [1], [2], we focused on **short-range communications**. In such cases, ultra-low transmission power and low-complexity implementation are required. As discussed in Sec. IV, for very short distances, molecular absorption loss is almost negligible. Therefore, the THz band exhibits itself as almost a 10-THz-wide window. To make the most out of this bandwidth with minimal complexity, we proposed the utilization of one-hundred-femtosecond-long pulses. Such pulses are transmitted by following an on-off keying modulation and spreading the symbols in time (TS-OOK) [167], [168]. In TS-OOK, 1s and 0s are transmitted as pulses and silence, respectively, which drastically simplifies the transmitter and the receiver architecture. Moreover, TS-OOK aims to further relax the hardware requirements and enable uncoordinated multiplexing of parallel streams between different users. To this end, instead of being sent back to back, symbols are spaced out in time to avoid temporal broadening effects (as elaborated in Sec. IV-C) and allow for multiple access. In addition, TS-OOK just detect binary information. Benefiting from this, the PHY overhead is shorter, compared to the commonly used phase-shift keying (PSK) and quadrature amplitude modulation (QAM) [16]. Besides the TS-OOK reducing the PHY overhead, an index modulation has been applied to assist the THz pilot design with shorter codewords [169]. Specifically, this method maps the indices of data and pilot subblocks onto short index bits with the logarithmic length.

When increasing the communication distance to **macro-/micro-scale**, the distance-dependent bandwidth of the THz band created by molecular absorption needs to be accounted for. In this direction, in [170], we proposed the utilization of multiple transmission windows, each on its turn with a variable number of narrower-band pulses. More specifically, by ensuring the data rate demands, the optimal waveform design is proposed to determine the transmit power and sub-window rate. THz communication distances can thereby be maximized with thorough consideration of multiple peculiarities of THz waves, including the distance-varying spectral windows, the delay spread, as well as the temporal broadening effects. More recently, in [171], we have introduced the concept of hierarchical bandwidth modulations (HBMs). The goal of HBM is to simultaneously transmit independent data streams to multiple users at different distances within the same transmission beam. To this end, HBMs dynamically exploit the distance-dependent bandwidth of the THz band and multiple modulation constellations of all the users. More specifically, HBMs build on top of traditional hierarchical or

concatenated modulations [172]. Users are able to recover different information based on their perceived signal-to-noise ratio (SNR). As a result, users at different distances can utilize a different bandwidth. The atmospheric loss issue is hence turned into an opportunity of the utilization maximization for distance-dependent THz bandwidth.

Innovative waveforms are needed to support **ISAC** [14]. Several attempts have been recently reported. First, we have applied non-uniform subcarrier spacing and superposition to multiple orthogonal frequency division multiplexing (OFDM) waveforms, and the sensing accuracy is dramatically improved, and the throughput is enhanced [173]. Besides multi-carrier design, we have presented a single-carrier study in [174], in which we proposed a sensing integrated discrete Fourier transform spread orthogonal frequency division multiplexing (SI-DFT-s-OFDM) to explore the distinct peculiarities of sensing and communication channels. Simulation results illustrate that SI-DFT-s-OFDM realizes ten times higher estimation accuracy, compared to the conventional OFDM. Third, a new modulation technique named orthogonal time frequency space (OTFS) was recently proposed to address high Doppler spread in doubly selective channels [175]. OTFS maps the information symbols on the delay-Doppler domain, which provides a sparse representation of a time-varying multipath channel. To unleash the potential in the THz band, we have developed a discrete Fourier transform spread OTFS (DFT-s-OTFS) modulation scheme for THz communications in [176], which can achieve strong robustness to Doppler spread compared to OFDM/DFT-s-OFDM and provide lower peak-to-average power ratio (PAPR) in contrast with OTFS. This design could be further explored to include the sensing function.

In addition to novel modulation schemes, customized coding designs for THz communications are proposed. For instance in IEEE 802.15.3d [16], the header check sequence (HCS) is exploited to ensure the correctness of the PHY and MAC headers for THz signals. The robustness is enhanced by encoding HCS together with these headers through the extended Hamming code. Pertaining to the OOK modulation, IEEE 802.15.3d suggests the Reed Solomon code to realize hard-decision yet simple binary decoding in addition to the low-density parity-check (LDPC)-based methods.

Moreover, effective next-generation forward error correction (FEC) schemes are required to resolve the channel errors in the THz band. Motivated by this, it is essential to know the nature of such errors by developing stochastic models of noise, multipath fading, and interference first. Then, with the knowledge of errors, advanced state-of-the-art error control policies such as turbo, LDPC, and polar codes can be the potential candidates to be implemented in the THz band. Rather than adopting existing coding schemes, ultra-low-complexity channel coding schemes are also favored as excellent solutions for THz communications. More specifically, such schemes can preclude channel errors instead of correcting them afterward. For example, for short-range communications, with femtosecond-long pulse-based modulations, we have successfully applied low-weight coding schemes [177], [178]. In the future, these FEC technologies need further validation and demonstration on a

practical THz chipset.

B. Dynamic Hybrid Beamforming

As discussed in Sec. III, owing to the sub-millimeter wavelength of THz signals, very-large-scale antenna arrays can be applied. For instance, 1024, 4096, and even more antenna elements can be integrated on the antenna arrays for a transceiver. As a result, the promising ultra-massive multiple-input-multiple-output (UM-MIMO) systems can be achieved. On one hand, such systems can achieve high beamforming gains, which combat the short transmission distance problem incurred by the high path loss. On the other hand, multiplexing gains can be realized to further improve spectral efficiency by transmitting multiple data streams simultaneously.

Instead of conventional analog and digital beamforming architectures that are limited by performance and hardware constraints, hybrid beamforming is appealing in the THz band [102], [179]–[184]. Specifically, in the hybrid structure, signal processing is divided into a digital baseband and a radio-frequency (RF) part through a phase shifter network. As illustrated in Fig. 10, hybrid beamforming can be further classified into three categories, namely, fully-connected, array-of-subarray (AoSA), and dynamic AoSA architectures. As dynamically structured hybrid beamforming, the third architecture proposed in our previous work can reach a balance among good spectrum efficiency, low hardware complexity, and energy efficiency [185]. Moreover, this dynamic structure intelligently customizes the connections between RF chains and subarrays via a network of switches, to evolve as the fully-connected and AoSA counterparts. To realize this, on the one hand, each of subarrays connects to a unique RF chain through a set of switches. On the other hand, the authors in [186] propose to connect each subarray with multiple RF chains via a combiner.

Practical design has been recently proposed to adopt quantized phase shifters and even fixed phase shifters to replace the infinite-resolution phase shifters that are costly with high hardware complexity. As shown in Fig. 11, we have devised the dynamic hybrid beamforming with quantized phase shifters that operate discrete phases [187]. This system realizes 36% energy efficiency enhancement at the expense of only 2% spectral efficiency, compared to the scheme with infinite-resolution phase shifters. Moreover, by equipping with more economical fixed-phase shifters, the dynamic hybrid beamforming can further achieve 30% more energy efficiency than that with quantized-phase shifters [187]. However, 21% reduction in terms of the spectral efficiency comes at the price.

In the THz UM-MIMO systems, with broad bandwidth and very large antenna array, a beam squint problem arises since the phase shifter cannot generate frequency-proportional weights. Fortunately, the beamforming weights generated by true-time-delay (TTD) is frequency-proportional and can be used to solve beam squint. Hence, hybrid beamforming using TTD for phase adjustment is a promising alternative to address the wideband beam squint problem in the THz band, while offering high array gains [188]. As one step further, we propose a novel dynamic-subarray with fixed true-time-delay

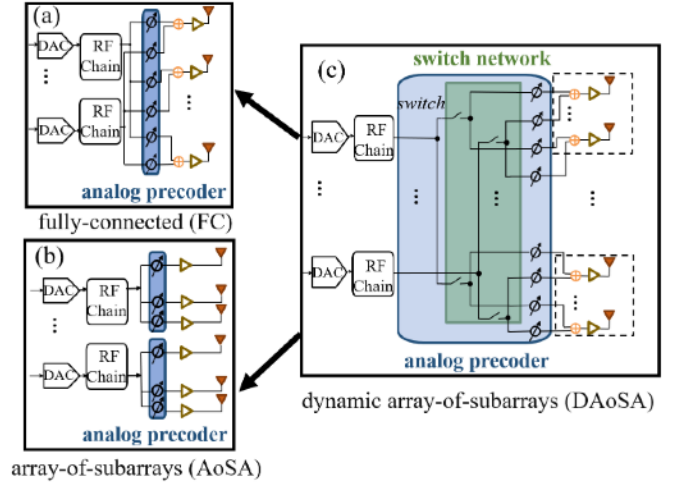


Fig. 10. Three hybrid beamforming architectures for THz communications, namely, (a) fully-connected (FC), (b) array-of-subarray (AoSA), and (c) dynamic AoSA

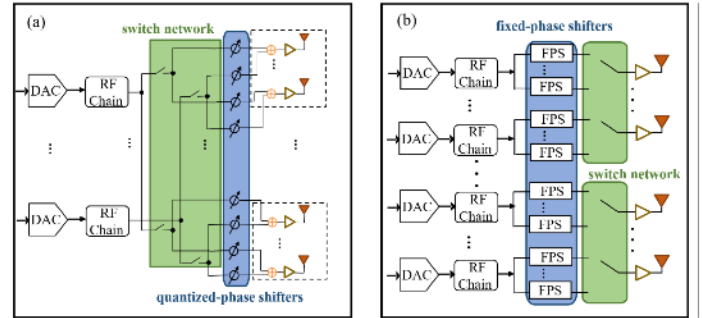


Fig. 11. (a) Dynamic hybrid beamforming architecture with quantized-phase shifters, (b) Dynamic hybrid beamforming architecture with fixed-phase shifters.

(DS-FTTD) architecture in [189], which owns lower power consumption and hardware complexity, thanks to the low-cost FTDDs.

C. Beam Estimation and Tracking

As a key of beam management, beam alignment that involves angle estimation and tracking is critical. Mainly, *on-grid* and *off-grid* methods are categorized in the literature for beam estimation and tracking. On the one hand, on-grid methods utilize predetermined spatial grids to estimate the DoA, for which the accuracy is thereby dependent on the grid resolution [190], [191]. As downside, to reach the desired resolution, the on-grid schemes suffer from high complexity and large beamforming training (BFT) overhead. On the other hand, off-grid methods perform subspace-based super-resolution DoA estimation or discard the fixed angular grids. To support the super-resolution DoA estimation for the aforementioned subarray-based hybrid beamforming structure, we have proposed a THz-specific AoSA-multiple signal classification (AoSA-MUSIC) in [192]. Simulation results demonstrate its ability to realize millidegree-level angle estimation and millisecond level tracking. In addition, a variant of subspace

pursuit (SP) algorithms in compressed sensing (CS) is also utilized to estimate the angle of beams with low computational complexity for THz MIMO systems [193]. Moreover, a major challenge of beam estimation relates to the beam squint problem, or the so-called triple delay-beam-Doppler squint effects. To tackle this, a variant of the traditional orthogonal matching pursuit (OMP) is exploited to solve the CS problem [194]. Moreover, the authors in [195] study the estimation and tracking of fine beam angles in space-air-ground networks.

Besides the above methods, an innovative beamforming architecture that utilizes the beam squint effect can, in turn, inspire the design of beam estimation and tracking. When transmitting THz wideband signals, the time delay elements can also make phase shift frequency-dependently, which is called THzPrism [196]. This property makes the phased array radiate different frequency carriers to diverse directions and remarkably broaden the angular coverage. For example, THzPrism-based hybrid beamforming achieves 124% more data rate, serves 147% more users, while consuming 71% less power than the existing approaches [197]. With such a structure, multiple beams can be generated and utilized simultaneously for tracking, based on the pairing between frequency and beam angle [198]. Specifically, accurate tracking results are obtained with 90% less overhead, compared to the counterpart hybrid beamforming architectures.

Thanks to the recent rapid development of DL for wireless communications, inherent attributes of channels such as angle information can be excavated via DL-based methods. For example, we have deployed a deep convolutional neural network (DCNN) in THz networks, and the beam estimation is enhanced in terms of both accuracy and complexity [199]. Besides, we have further developed DCNN as well as the convolutional long short-term memory (ConvLSTM) for beam estimation and tracking, respectively [200]. DCNN outperforms non-learning methods under high SNR, while ConvLSTM can realize the accuracy on the order of 0.1° at a millisecond (ms) level with 50% reduced overhead. Thus, DL-based methods are promising to reach higher efficiency and accuracy in complex THz wireless environments, which still needs further research efforts.

D. Synchronization

According to the Nyquist sampling theorem, sampling the received signal and performing sophisticated digital signal processing are quite challenging to meet Tbps transmission rates. Novel designs for synchronization is thereby motivated. Aiming at realizing the efficient synchronization in THz systems, our solution determines the symbol start time and shortens the observation window iteratively [201]. This solution achieves the tight synchronization with a low symbol error rate and a few preamble bits under the pulse-based modulation. Besides, by jointly exploiting one receiver-initiated handshake mechanism and the aggregated packet or sliding window flow control, we have proposed a synchronization method in [202]. This method is applicable to the carrier-based scenarios apart from the pulse-based modulation. Furthermore, to realize the sub-Nyquist sampling, we extended the sampling theory with

finite rate from compressive sampling to the communication context [203].

In addition to timing acquisition, robust and comprehensive synchronization mechanisms for carrier frequency and phase are needed as well. Since the correlation between beam domain channel elements and time/frequency vanishes gradually with more antennas at transceivers in mm-wave/THz MIMO systems, separate synchronization for each beam is developed in [154] to exploit this phenomenon.

E. Localization

Accurate localization is required for 6G and Beyond wireless systems. With the ultra-broad bandwidth of the THz band, the localization performance is expected to reach 50 centimeter outdoor, 1 centimeter indoor, as well as 1–3 mm imaging resolution [204], [205]. Recent attempts commence on the low-cost THz backscattered systems. Specifically, in such systems, the reader devices radiate signals, and the passive tag devices modulate and reflect part of the signal back to the reader. Following this direction, systems based on chipless radio frequency identification (RFID) have been developed to solve the indoor localization with millimeter-level accuracy [206], [207]. In particular, the tags with known geographic positions are served as the reference, and the reader predicts its own position on the basis of the backscattered signals. Besides the indoor localization, we have implemented the THz backscattered communications to localize the in-body bionanosensors [208]. In this system, in-body bionanosensors deploy inertial measurement units (IMUs) with nanoscale accelerometers and gyroscopes. Such units enable the sensors to leverage the inertial positioning, and then the operator collects the position information through the resource-efficient THz backscattered links.

Apart from the backscattered systems, an innovative cooperative localization scheme has been proposed in [209] for complex three-dimensional indoor environments, e.g., office and laboratory. Particularly, multiple base stations, each of which performs an AoA tracking, cooperate with each other and increase the localization accuracy with low-estimation overhead. In addition, we have specifically designed recurrent neural networks exploring multiple features, including power, 3D AoA, and ToA, of all the MPCs from multiple transmitters [210], [211]. This neural network enhances the accuracy of the indoor localization to centimeter-level in complex indoor environment, which needs further improvement to reach the goal of millimeter-level accuracy.

F. Physical Layer Security

Besides the enticing data rate owing to the abundant bandwidth resource, the potential of physical layer security of THz communications needs in-depth analysis. Indeed, the potential of THz communications for enhancing information security has attracted great attention due to its high directivity and high path loss [212]–[214]. Although owing to the high directivity in THz systems, the probability that eavesdroppers locate in the beam sector of the legitimate transmission is low, the security of THz communications is

still an essential issue for the following three reasons. First, as long as the eavesdropper is inside the beam sector for the legitimate communication, the directivity of THz beams fails to bring security. Second, signals can be intercepted by an object laying on the LoS paths and scattered towards the eavesdropper [212]. Third, the multipath-based method or circumventing eavesdropping [215], [216] can reduce the eavesdropping probability and increase the secrecy rate. These reasons motivate the exploration of novel countermeasures of physical layer security.

To start with, security schemes that consider the special attributes of the ultra-spread THz spectrum can be investigated. To this end, we have devised a distance-adaptive absorption peak modulation (DA-APM) scheme in [217]. The main principle is to utilize the frequency-dependent molecular absorption, and the solution is based on spectrum management, by selecting frequency bands with proper molecular absorption coefficients. As a result, the eavesdroppable area is largely shrunk although both eavesdropper and receiver reside in the beam sector of the transmitter. Nevertheless, this scheme is valid only when the eavesdropper is farther than the legitimate receiver.

On the contrary, in the case of eavesdroppers in close proximity where eavesdroppers are nearer from the transmitter than the legitimate user, a widely-used idea is to simultaneously transmit artificial noise (AN) signals. The AN signal does not contain information, which is sent together with information signals to confuse the eavesdroppers. Most existing studies have suggested the transmitter to generate AN signals, which nevertheless are not applicable for THz LoS transmission, since the LoS path is shared between the legitimate user and the eavesdroppers. Instead, we have proposed a molecular absorption aided receiver AN scheme in the THz band, where the expensive self-interference cancellation (SIC) is not needed [218]. The key idea is to design the information and AN waveforms based on the temporal broadening effect caused by molecular absorption (as discussed in Sec. IV-C). Specifically, the higher molecular absorption of THz waves at a longer distance can lead to more severe pulse broadening in the time domain. Based on this, the received signal detection period and constituent ratios of transmission periods (for sending both information signals and ANs) are cooperatively devised. Consequently, eavesdropping is prevented by the receiver AN scheme, while legitimate communication is guaranteed.

G. Open Problems

- **PHY Solutions for Terahertz Integrated Sensing, Communication, and Intelligence (ISCI).** On the one hand, an integration of THz sensing and communication enables simultaneous message transmission and environment perception with shared spectrum, hardware, signal processing modules. On the other hand, driven by ubiquitous signal streams and sensing data, AI can mine the information and further empower the wireless system. PHY solutions for the THz ISCI need to be developed from the following three aspects. First, related to the discussion in

Sec. V-A, sensing function needs to be incorporated in the modulation and waveform design, With multiple objectives including sensing targets and information transmission. Second, beamforming technologies that balance the tradeoff between communication and sensing need to be developed, due to the distinction of their objectives. That is, sensing prefers scanning beams to search targets, while communication requires stable beams toward receivers. Third, AI methods can address the imperfections and non-linear distortion of THz transceivers. As a result, signal detection, sensing parameter estimation, and even an integrated detector based on AI algorithms are promising for THz communication systems [204].

- **Inter- and Intra-path Multiplexing Hybrid Beamforming.** In contrast with the lower-frequency MIMO systems that are constrained by the number of antennas, the multiplexing gain of the UM-MIMO system is instead limited by the spatial degree-of-freedom of the THz sparse channel. To this end, an idea to explore additional intra-path multiplexing gain is to enlarge the antenna or subarray spacing, and thereby form the widely spaced multi-subarray (WSMS) architecture [219], [220], which is also known as LoS MIMO [221]. In the WSMS architecture, the antenna array is composed of multiple subarrays, in which the antenna spacing is half of the wavelength. By contrast, the subarrays are widely-spaced. Each subarray observes the same propagation path with different angles, for which spherical-wave propagation needs to be accounted for. As a result, one propagation path between transmitted and received arrays can be decomposed into multiple sub-paths at the subarray level, which enhances the degree-of-freedom and brings additional intra-path multiplexing gain.
- **Joint Active and Passive Beamforming.** As mentioned in Sec. III-C, RIS-embedded THz systems have the potential to alleviate the LoS blockage issue as well as to enlarge the coverage, by intelligently controlling the incident wave reflection [222]. Multiple research problems still remain, including the joint design of active and passive beamforming algorithm in the THz band. On one hand, the active beamforming enabled by antenna array systems takes advantage of the small size and large integration of THz antennas. By concentrating the transmission energy to radiate towards users, the receiving power and transmission coverage can be considerably improved. On the other hand, the RIS is equipped with a metamaterial surface of the integrated circuit, which can be programmed and customized to generate passive beamforming to control the reflection of the incident wave from the transmitting end to the target user and effectively bypass the barrier and increase the selection of transmission routes [223], [224].

VI. HIGHER LAYER NETWORKING PROTOCOLS

6G and Beyond wireless systems require efficient end-to-end solutions, not only at the physical layer. The distinct device technologies in Sec. III and attributes of THz waves

elaborated in Sec. IV-C motivate rethinking the higher layers of the protocol stack. In this section, we investigate the innovative designs for the data link layer and network layer. More specifically, we focus on medium access control (MAC) design, interference, and coverage in the data link layer. For the network layer, we discuss relaying, routing, and scheduling.

A. Medium Access Control

The characteristics of THz communications pose the following challenges on MAC design [225]. First, the need for high-gain directional antennas (and, thus, narrow beams) simultaneously at the transmitter and the receiver makes link-layer synchronization extremely challenging due to the deafness problem. First, users need to discover their neighbors, a process that can be highly resource consuming when very narrow beams are used and no separate control channel exists. Second, even when the nodes have situational awareness, they need to be facing each other, which again cannot be easily ensured with traditional coordination solutions. Third, due to various human or wall LoS blockages, the cell boundary determined by the received signal strength (RSS) can be not regular circular or hexagonal. Instead, the shape of boundary might become amorphous.

There have been several MAC protocols recently proposed to address these challenges [226]. To solve the deafness problem in a more timely and less energy consuming approach than traditional beam search algorithms, we have proposed the use of receiver-initiated MAC protocols [202]. With such protocols, users periodically sweep space following a predefined pattern to ensure that all nodes can find each other. The very high data-rates of THz communications then enable ultra-fast data transmission during the communication period for each pair of nodes. To accelerate the neighbor discovery, the authors in [227] exploit the THz rainbow to obtain the angular information of users. In particular, the THz rainbow is created by using a leaky waveguide, and the entire angular space is thus illuminated with different THz frequencies. The neighbor angular location and rotation information are then acquired on the basis of the specific frequency of the received spectrum. Similarly for network association and neighbor discovery, we have exploited side lobe information of highly THz directional antennas, which is promising to accelerate the neighbor discovery [228]. Moreover, to carefully design the control signaling, we have leveraged the microwave radio for the exchange of very short control frames to schedule THz transmissions [229], [230]. Specifically, 2.4/5 GHz omnidirectional radio is utilized for control signaling, while THz beamforming is adopted for data transmissions. As a result, THz communication networks are potential to reach the lower delay, higher throughput than existing MAC protocols. In line with this idea, joint optimization of triple types of radio (THz, mm-wave, and microwave) for concurrent unidirectional data and control signal transmissions is analyzed in [231].

Recently, we have proposed the use of non-orthogonal multiple access (NOMA) in THz networks as well, with the goals of improving spectral efficiency and promoting fairness

across users, especially for the weak user in a network [232]. The key principles of NOMA are to utilize the power domain and exploit the channel difference of users, in which successive interference cancellation is equipped at the strong user in the NOMA pair. In light of this, maximization of throughput and energy efficiency can be realized by optimizing the utilization of beam, bandwidth, and power resources with guaranteed fairness [233], [234].

To relate MAC with resource allocation, we have proposed an interesting yet unique idea for the THz spectrum in [235], which exploits the distance-aware and bandwidth-adaptive features and is known as long-user-central-window (LUCW). Specifically, benefited from the distance-adaptive modulations as discussed in V-A, the LUCW principle intelligently allocates the center spectrum of the spectral windows to the long-distance users first, and then the side spectrum to the short-distance users [160]. We further develop this multi-band-based spectrum allocation idea with adaptive sub-band bandwidth by allowing the spectrum of interest to be divided into sub-bands with unequal bandwidths [236].

B. Interference and Coverage

The use of high-gain directional antennas at all times requires revisiting some of the well-established multi-user interference and coverage models. As we first analyzed in [237], the interference on a user residing within the main transmitter beam is extremely high, due to the very high antenna directivity gain. However, the probability of having an interfering user within the main transmit beam is very low. We derive the moment generating functions of the aggregated interference and theoretical expressions for the mean interference power in [238]. Compared to the RF and mm-wave communications, interference strength in THz directional transmission is much weaker on average.

On the downside, directional beams lead to a significant beam misalignment problem (as elaborated in Sec. V-C) that lessens the coverage and communication quality in THz networks. Although dense networks could help coverage enlargement, the expense is the increasing interference as we analyzed in [32]. To this regard, multiple analysis of coverage in THz networks have been conducted. Based on the aggregated interference and theoretical expressions for the mean interference power, we have derived the approximated coverage probability and average network throughput [238]. Numerically, AP density of $0.15/\text{m}^2$, i.e., one AP per 6.7m^2 , is recommended to support 93% coverage probability and 30 Gbps/ m^2 network throughput. Apart from the consideration of indoor blockage, we have investigated an accurate coverage model taking into account the 3D property of THz communication [239]. Simulation results demonstrate that increasing the antenna directivity at APs rather than UEs is more efficient to enhance the reliability of THz communications. By contrast, the accurate coverage analysis with outdoor LoS blockages for THz communications is studied as well [240], showing that denser nodes, longer transmission distance, lower latitude and more humid seasons result in lower coverage probability and narrower transmission windows.

Recent research efforts have been made to suppress the interference and enhance the coverage. As for the interference mitigation, the aforementioned LUCW and the flexible distance-aware scheme [241] can achieve massive connection while preventing interference. Combined with reinforcement learning, adaptive intermittent interference detection and mitigation in dynamic THz channels are achievable as well [242]. By contrast, without incurring severe inter-symbol interference, we have illustrated that the multiple access points can remarkably increase the coverage probability [243]. In particular, with the output power of 1 W, as the number of access points increases from 1 to 20, the coverage probability rises from 25% to 95%, respectively. To further improve the coverage probability, we propose the nearest LoS-AP association that is promising to outperform the traditional nearest AP association [238].

C. Multi-hop Communications with Active and Passive Relays

Multi-hop scheme is useful to extend the coverage, by using active and passive relays. On the one hand, by repeating or even amplifying the received signals along transmission paths, relays can combat the distance limitation of the THz propagation. On the other hand, relays can be leveraged to circumvent the obstacles, forming multiple segments of LoS paths.

Owing to these advantages, we have implemented a multi-hop scheme to realize the nanoscale THz communication networks [244]. In particular, this design enlarges the transmission coverage that is limited by the constrained transmit power in nano-devices. In macro- or micro-scale THz networks, we have derived a mathematical model to explore the optimal distances between relays in [245]. More specifically, the effects of THz directional antennas from the perspectives of all the physical, link, and network layers are jointly considered. Another research direction is on customizing the directions of transmitting for each relay. To this end, the authors in [246] derive the closed-form expressions for the THz two-way relay hybrid precoding optimization. Furthermore, we illustrate that thanks to the broad THz spectrum resource, efficient transmission among multiple wireless hops enables the integrated access and backhaul (IAB) [247]. Hence, wireless relays in IAB can reduce the cost of wireline connections among base stations, while the IAB topology and signal routing need to be further investigated.

In addition to these active relays (e.g. transceivers), we have employed energy-efficient passive beamforming for the intelligent surfaces (detailed in Sec. III-C) in a multi-hop network [248]. For example, simulation results illustrate the feasibility and advancement of multi-hop THz RIS assisted networks, compared to single-hop systems and those without RIS [249]. Specifically, the management of direction is supported by deep reinforcement learning (DRL) to achieve the optimization for NP-hard hybrid beamforming.

D. Routing and Scheduling

Inherited from previous analysis on multi-hop THz networks in Sec. VI-C, efficient routing mechanisms are needed to

realize high throughput, low relay, and high reliability, among others. Indeed, the special THz channel molecular composition and its impact on the available distance-dependent bandwidth need to be considered when devising routing mechanisms. Moreover, with the growth of number of users in the dense network, the formidable optimization problem for routing and scheduling requires novel solutions, such as ML- and AI-enabled methods [204]. The aim is to learn and adapt real-time routing policy with guaranteed high overall network throughput. In line with this, we employ tabular reinforcement learning for routing protocol design, by considering the limited buffer size and directional THz signals [250]. Simulation results demonstrate a low buffer blockage rate and a high packet arrival rate could be achieved.

In nano-scale THz networks with a rather limited buffer size, we use reinforcement learning to demonstrate its capability to increase the packet delivery rate and lessen the hop count [244]. In the context of intra-body THz communication networks, the molecular adsorption can result in temperature rise and the risk of tissue damage. Aiming at precluding this effect, by estimating the temperature rise, a temporal correlation-based algorithm is proposed [251]. As a result, the temperature rise is dramatically mitigated by 75%-85% with high energy efficiency.

Scheduling that determines priority of packet delivery is worth being re-examined for THz networks with limited memory. We have proposed a distributed scheduling algorithm in [252] to achieve timely optimal throughput in THz bufferless IoNT. Particularly, the authors explore the future traffic rate, virtual debts, and channel sensing information captured by each wireless device. Perpetual communications can be achieved via the joint consideration of both energy consumption and harvesting. Furthermore, we suggest the idling energy should not be neglected, and design a new duty cycle for the receiving nanonodes to reduce the idling energy consumption as efficient scheduling in [253].

E. Open Problems

- **Effective and Efficient Design for Resource Allocation.** In dense THz networks with ultra-large concurrent user demands, joint optimization to ensure QoS needs effective and efficient allocation of diverse resources, including time, bandwidth, antennas, power, routes, among others. However, the non-convexity and NP-hardness usually challenge the joint designs if without loosening practical constraints. ML is favored as a candidate to solve such problems with its powerful learning ability. Nevertheless, the high complexity and large storage requirements should be addressed in online training and deployment for practical uses.
- **Transport Layer Protocols.** The wireless multi-Gbps and Tbps links can bring a tremendous boost of the aggregated traffic in the network. This significantly challenges transport layer design regarding congestion control as well as reliable end-to-end transport. For example, re-design of the transmission control protocol (TCP) congestion control window mechanism is necessary to handle the

traffic dynamics of THz networks. We demonstrate that under ideal MAC schemes, THz TCP can reach very high data rates [32]. However, with realistic MAC schemes, the interplay between the contention-based access and the TCP timers is inefficient. Transmissions thereby suffer recurrent timeouts and congestion recovery. Motivated by this, further investigation of efficient networks and transport protocols for THz links is needed to guarantee end-to-end reliability.

- **Cross Layer Design.** The ultra-high data rate in THz communications and super-low end-to-end latency requirement by many applications in 6G networks. Hence, simplifying interactions across protocol stacks becomes significant yet urgent. A promising approach is to merge the network and transport layers with the link and even physical layers, designing cross-layer solutions. Such solutions, including our previous work [254], are expected to not only improve the efficiency of the protocol stack, but achieve joint optimization among PHY, MAC, routing, and transport functions as well.

VII. EXPERIMENTAL AND SIMULATION PLATFORMS

Ten years ago, the research on THz communications was mostly theoretical. Today, thanks to the advancements in the device technologies (Sec. III), THz research is quickly transitioning from theory to practice. In this section, we describe existing THz experimental platforms as well as state-of-the-art simulation and emulation software, which serves as an intermediate step between pure theory and experimental research.

A. Technology Demonstrators and Communication Testbeds

We can classify experimental platforms in three categories based on their capabilities: channel sounding systems, technology demonstrators and communication testbeds. Channel sounding systems, which we have already described in Sec. IV-A, implement no physical layer (in the case of VNA or THz-TDS systems) or a very limited physical layer that supports only the transmission of channel sounding sequences (in the case of time-domain correlators). In this section, we focus on systems that implement at least a physical layer.

Technology demonstrators are platforms that have been used to experimentally demonstrate the practicality or capabilities of a specific hardware configuration or physical layer solution and, as such, provide limited reconfigurability. A detailed survey shows that lab-level technology demonstrators can be realized in two ways [255]. On one hand, an approach named the solid state THz system generates THz signals by processing the intermediate frequency modulated sources. On the other hand, the high-power THz signal can be directly generated by the direct modulation THz system.

Some of the very early technology demonstrators date back more than ten years, such as the Schottky-diode-based transmission system at 300 GHz first introduced in [256] and later upgraded in [257], which supported fixed analog and digital video transmission, respectively. Similarly, as a

demonstrator of the capabilities of UTC-based photonic transmitters, operating in conjunction with a Schottky-diode-based electronic receiver, a system able to support first 12.5 Gbps and later 24 Gbps at 50 cm was shown in [258] and [259], respectively. Going up in frequency, a system able to operate at 625 GHz based on again Schottky diodes was shown in [260], with 2.5 Gbps. The integration of the THz electronic hardware components in a single Terahertz Monolithic Integrated Circuit (TMIC) has also enabled the development of more compact THz systems, such as those presented in [261]–[266], generally in the sub-300 GHz range (with the exception of [265] at 666 GHz), with data-rates of up to 100 Gbps [263] and distances of up to 850 m [264].

In the recent years, the photonics approach is becoming more aggressively pursued. Particularly, up to 106 Gbps links have been realized by a photonic-wireless communication system operating at 400 GHz [267]. By utilizing the technique of orthogonal polarization dual antennas, the upgraded system has achieved more than 2×300 Gbps throughput with two channels [268]. Designed for a 2×2 MIMO link, another photonics-based THz system has demonstrated a 6×20 Gbps data rate as well, with the frequency ranging from 375 GHz to 500 GHz in six channels [269]. In addition to the photonics-aided transmitter, by deploying analog down-conversion through an electrical mixer at the receiver side and electrical-to-optical conversion via direct modulation, up to 13 Gbps fiber-THz-fiber communication has been realized at 450 GHz [270].

Customized solutions for specific applications have also been presented. For example, the first functional demonstrator for THz kiosks, aimed at transferring a large amount of data from a stationary terminal to a mobile wireless device in a very short time under the “touch-and-go” scenario, has recently been demonstrated in [271]. In this platform, InP-based front-ends at 300 GHz are utilized in conjunction with a high-speed field programmable gate array (FPGA)-based physical layer that implements Reed-Solomon (RS) FEC to demonstrate 20 Gbps of real-time data. Another specific application, in which THz communications play a key role, is uncompressed high-definition (HD) (60 fps) and 4K (30 fps) video transmission. In [272], a UTC-based photonic transmitter is utilized in conjunction with a Schottky-diode-based receiver at 138 GHz to demonstrate video transmission over 30 cm with 99% of undamaged frames in HD and 95% in 4K.

The goal of **communication testbeds** is to facilitate the testing of new communication solutions for ultrabroadband networks in the THz band. As such, a testbed should be highly reconfigurable and easy to reprogram to support different hardware blocks, signal processing algorithms, or communication and networking protocols. In this direction, in [273], [274] we introduced the *TeraNova* platform, the world’s first integrated testbed for ultrabroadband communication networks in the THz band. The highly modular testbed consists of several analog up & down converting front-ends at 120–140 GHz, 210–240 GHz and 1–1.05 THz, making it not only the highest frequency platform existing to date, but also multi-band. The front-ends can be interfaces to different available DSP back-ends able to process baseband bandwidths ranging from 2 GHz in real-time

and up to 32 GHz offline, per channel. Directional antennas with gains ranging from 21 dBi to 55 dBi are available at the different frequencies. The TeraNova platform supports the development of 6G THz systems in many ways, including but not limited to: 1) ultra-broadband channel sounding in indoor and outdoor scenarios; 2) design of ultra-broadband synchronization, channel estimation and equalization, modulation and coding; and, 3) testing of directional medium access control, neighbor discovery, and multi-hop relaying. Remote access is also supported. Some of the early data-sets collected with the testbed are available in SigMF format [275].

Major equipment vendors have also recently entered the arena above 100 GHz. In [276], National Instruments (NI) exemplifies how their mm-wave transmitter systems (MTS) can be extended to operate above 100 GHz by directly connecting their FPGA-based baseband to THz up & down converters. The MTS supports different functionalities, including channel sounding as well as pre-defined TDMA-type and OFDM-type physical layers. In [277], Keysight Technologies demonstrate how their commercial signal generators, arbitrary waveform generators, signal analyzers and digital storage oscilloscopes can be used for testing of hardware components, channel models and signal processing algorithms, when combined with up & down converters above 100 GHz. Interestingly, both vendors as well as many of the aforementioned electronic-based THz systems rely on frequency up & down converters built by Virginia Diodes Inc. [278].

B. Simulation Tools

In parallel to the development of experimental testbeds, simulation tools are needed to expedite the development of communication and networking protocols tailored to THz systems, at a fraction of the cost. Simulation platforms can be categorized into propagation/channel simulators and communication/networking simulators.

Channel simulators are aimed at reducing the costly and time-demanding process of collecting extensive data sets for different scenarios with changing geometry, weather conditions, etc. With generalized parameters extracted from measurements, channel simulators can virtually approximate wireless propagation models on demand. Different options are available to date. Commercial software, such as EDX Advanced Propagation and Wireless InSite can be utilized at frequencies up to 0.1 THz [279]. Academia-driven platforms, such as *CloudRT* developed by BJTU and Technische Universität Braunschweig, supports the simulation of both urban indoor and outdoor cases at 450 MHz-325 GHz [279]. Ad-hoc channel solvers that build on experimentally-measured data have been utilized to explore the performance of different specific scenarios, including THz backhaul links at 300 GHz [280] or multimedia kiosks [281]. While many of the existing platforms are for single channel simulators, *TeraMIMO* [282] has been recently developed to simulate UM MIMO channels in 3D scenarios, capturing the properties described in Sec. V. Other simulation platforms, such as [283], are being developed with the aim of not only simulating the channel, but also testing certain physical layer solutions.

While at a lower pace than channel simulators, THz **network simulators** are also being developed. THz network simulation tools are designed with the objective of testing, refining and optimizing networking protocols for THz networks, such as those described and envisioned in Sec. VI. Aimed at the simulation of nanoscale THz communication networks, *Nano-Sim* was first introduced in [284]. *Nano-sim* is built as an extension to *ns-3*, which is one of the most widely used teaching and education network simulation software, and incorporates a simplified channel model for ultra-short range THz communications and a tailored protocol stack. More recently, in [285], we introduced *TeraSim*, an open source network simulation platform for THz communication networks that is also built as an *ns-3* extension and it is officially available in the *ns-3* App Store. The simulator has been developed considering two major types of application scenarios, namely, nanoscale communication networks and macroscale communication networks. The simulator consists of a common channel module that accurately captures the physics of the THz channel, separate physical and link layers tailored to each scenario, and two assisting modules, namely, THz directional antenna module and energy harvesting module, originally designed for the macroscale and nanoscale scenario, respectively. *Terasim* seamlessly interfaces with existing *ns-3* modules, including higher layer protocols and mobility models. Since its release in 2018, different groups have adopted *TeraSim*, and extended new capabilities, such as the inclusion of the latest experimentally-validated multi-path THz channel models [286].

VIII. CONCLUSIONS

THz communications are envisioned as a key technology for 6G and Beyond. The very large available bandwidth at THz frequencies (tens of GHz and more, i.e., two orders of magnitude more than that in the 5G systems) will drastically improve the performance of common network applications enabling Tera-WiFi, Tera-IoT, Tera-IAB; whereas the very small wavelength of THz waves opens the door to the new world of nanoscale electromagnetic communications networks such as IoNT, and WiNoC. Furthermore, by integrating the functions of sensing and communication, the THz ISAC applications include THz VR/AR, and vehicular communication and radar sensing.

Building on over ten years of research, in this paper, we have surveyed the recent advancements and highlighted the open research directions of THz communications, with the following take-away lessons. First, the THz technology gap is almost filled, thanks to the recent progress on THz device technologies, in particular that made in the last decade. However, still meaningful challenges remain related to both analog RF & digital hardware as well as integrated circuits at THz frequencies. Second, the propagation and channel modeling attract much attention to discover the spectrum peculiarities. Although recent efforts in indoor channel measurement at 140 GHz, 220 GHz, 300 GHz are reported, extensive studies are still needed at higher frequencies in various indoor and outdoor environment as well as less traditional

realms, including intra-body or space. Third, in terms of communications and signal processing, major challenges are to combat the distance limitation, reduce power consumption and support mobility coverage, by revisiting and inventing new techniques to make the most use of the broad bandwidth. Fourth, in THz networks with narrow beams, bandwidth is indeed no longer a constraint. Nevertheless, challenges are faced in medium access control, interference and coverage, multi-hop communications, routing and scheduling. Fifth, THz band interests not only to communications, but also to other scientific communities including sensing, imaging, astronomy, among others. Therefore, policy and regulation need to be made for efficient coexistence. Finally, although there is a standard for point-to-point links, great efforts and competitions are foreseen in the next a few years in 3GPP and ITU on THz communication standardization.

REFERENCES

- [1] I. F. Akyildiz, J. M. Jornet, and C. Han, "Terahertz band: Next frontier for wireless communications," *Physical Communication*, vol. 12, pp. 16–32, 2014. **1, 2, 3, 6, 16**
- [2] I. F. Akyildiz, J. M. Jornet, and C. Han, "TeraNets: ultra-broadband communication networks in the Terahertz band," *IEEE Wireless Communications*, vol. 21, no. 4, pp. 130–135, August 2014. **1, 2, 3, 6, 16**
- [3] I. F. Akyildiz, A. Kak, and S. Nie, "6G and beyond: The future of wireless communications systems," *IEEE Access*, vol. 8, pp. 133 995–134 030, 2020. **1, 9**
- [4] H. Elayan, O. Amin, B. Shihada, R. M. Shubair, and M.-S. Alouini, "Terahertz band: The last piece of rf spectrum puzzle for communication systems," *IEEE Open Journal of the Communications Society*, vol. 1, pp. 1–32, 2019. **1, 3, 6**
- [5] T. S. Rappaport, Y. Xing, O. Kanhere, S. Ju, A. Madanayake, S. Mandal, A. Alkhateeb, and G. C. Trichopoulos, "Wireless Communications and Applications Above 100 GHz: Opportunities and Challenges for 6G and Beyond," *IEEE Access*, vol. 7, pp. 78 729–78 757, 2019. **1, 3, 6**
- [6] A.-A. A. Boulogeorgos, A. Alexiou, T. Merkle, C. Schubert, R. Elschner, A. Katsiotis, P. Stavrianos, D. Kritharidis, P.-K. Chartas, J. Kokkonen, *et al.*, "Terahertz technologies to deliver optical network quality of experience in wireless systems beyond 5G," *IEEE Communications Magazine*, vol. 56, no. 6, pp. 144–151, 2018. **1**
- [7] H.-J. Song and N. Lee, "Terahertz Communications: Challenges in the Next Decade," to appear in *IEEE Transactions on Terahertz Science and Technology*, 2021. **1**
- [8] T. W. Crowe, W. R. Deal, M. Schröter, C.-K. C. Tzuang, and K. Wu, "Terahertz RF electronics and system integration," *Proceedings of the IEEE*, vol. 105, no. 6, pp. 985–989, 2017. **1**
- [9] K. M. S. Huq, S. A. Busari, J. Rodriguez, V. Frascolla, W. Bazzi, and D. C. Sicker, "Terahertz-enabled wireless system for beyond-5G ultra-fast networks: A brief survey," *IEEE Network*, vol. 33, no. 4, pp. 89–95, 2019. **1**
- [10] V. Petrov, J. Kokkonen, D. Moltchanov, J. Lehtomaki, Y. Koucheryavy, and M. Juntti, "Last meter indoor terahertz wireless access: Performance insights and implementation roadmap," *IEEE Communications Magazine*, vol. 56, no. 6, pp. 158–165, June 2018. **1**
- [11] I. F. Akyildiz and J. M. Jornet, "The internet of nano-things," *IEEE Wireless Communications Magazine*, vol. 17, no. 6, pp. 58–63, Dec. 2010. **1, 7**
- [12] Q. H. Abbasi, A. A. Nasir, K. Yang, K. A. Qaraqe, and A. Alomainy, "Cooperative in-vivo nano-network communication at terahertz frequencies," *IEEE Access*, vol. 5, pp. 8642–8647, 2017. **1**
- [13] H. Elayan, C. Stefanini, R. M. Shubair, and J. M. Jornet, "End-to-end noise model for intra-body terahertz nanoscale communication," *IEEE Transactions on NanoBioscience*, vol. 17, no. 4, pp. 464–473, 2018. **1**
- [14] Y. Wu, C. Han, and Z. Chen, "Thz isci: Terahertz integrated sensing, communication and intelligence," *Proc. of International Conference on Infrared, Millimeter, and Terahertz Waves (IRMMW-THz)*, 2021. **1, 16**
- [15] C. Castro, "EU Has Granted Over €95 Million in Funding for 6G Research," <https://www.6gworld.com/exclusives/eu-has-granted-over-e-95-million-in-funding-for-6g-research/>, April 2021. **2**
- [16] V. Petrov, T. Kurner, and I. Hosako, "IEEE 802.15.3d: First Standardization Efforts for Sub-Terahertz Band Communications toward 6G," *IEEE Communications Magazine*, vol. 58, no. 11, pp. 28–33, 2020. **2, 16**
- [17] T. Kürner and A. Hirata, "On the impact of the results of wrc 2019 on thz communications," in *Proc. of International Workshop on Mobile Terahertz Systems (IWMTS)*, 2020, pp. 1–3. **2**
- [18] "IEEE ComSoc Radio Communications Committee (RCC) Special Interest Group (SIG) on: TeraHertz Communications," 2021. [Online]. Available: <https://sites.google.com/view/ieee-comsoc-rcc-sig-thz/home> **2**
- [19] I. F. Akyildiz, C. Han, and S. Nie, "Combating the distance problem in the millimeter wave and terahertz frequency bands," *IEEE Communications Magazine*, vol. 56, no. 6, pp. 102–108, 2018. **3**
- [20] R. Piesiewicz, T. Kleine-Ostmann, N. Krumbholz, D. Mittleman, M. Koch, J. Schoebel, and T. Kurner, "Short-range Ultra-broadband Terahertz Communications: Concepts and Perspectives," *IEEE Antennas and Propagation Magazine*, vol. 49, no. 6, pp. 24–39, 2007. **3, 6**
- [21] J. Federici and L. Moeller, "Review of terahertz and subterahertz wireless communications," *Journal of Applied Physics*, vol. 107, no. 11, p. 6, 2010. **3, 6**
- [22] K.-c. Huang and Z. Wang, "Terahertz terabit wireless communication," *IEEE Microwave Magazine*, vol. 12, no. 4, pp. 108–116, 2011. **6**
- [23] H.-J. Song and T. Nagatsuma, "Present and Future of Terahertz Communications," *IEEE Transactions on Terahertz Science and Technology*, vol. 1, no. 1, pp. 256–263, 2011. **3, 6**
- [24] T. Nagatsuma, G. Ducournau, and C. C. Renaud, "Advances in terahertz communications accelerated by photonics," *Nature Photonics*, vol. 10, no. 6, pp. 371–379, 2016. **3, 6, 7**
- [25] I. Mehdi, J. V. Siles, C. Lee, and E. Schlecht, "THz diode technology: status, prospects, and applications," *Proceedings of the IEEE*, vol. 105, no. 6, pp. 990–1007, 2017. **3, 6, 10**
- [26] C. Han and Y. Chen, "Propagation modeling for wireless communications in the terahertz band," *IEEE Communications Magazine*, vol. 56, no. 6, pp. 96–101, 2018. **3, 6, 12, 13**
- [27] D. Headland, Y. Monnai, D. Abbott, C. Fumeaux, and W. Withayachumnankul, "Tutorial: Terahertz beamforming, from concepts to realizations," *Apl Photonics*, vol. 3, no. 5, p. 051101, 2018. **3, 6**
- [28] K. Sengupta, T. Nagatsuma, and D. M. Mittleman, "Terahertz integrated electronic and hybrid electronic-photon systems," *Nature Electronics*, vol. 1, no. 12, p. 622, 2018. **3, 6**
- [29] S. Abadal, C. Han, and J. M. Jornet, "Wave propagation and channel modeling in chip-scale wireless communications: A survey from millimeter-wave to terahertz and optics," *IEEE Access*, vol. 8, pp. 278–293, 2020. **3, 6**
- [30] K. Tekbiyik, A. R. Ekti, G. K. Kurt, A. Gorcin, and H. Yanikomeroglu, "A holistic investigation of terahertz propagation and channel modeling toward vertical heterogeneous networks," *IEEE Communications Magazine*, vol. 58, no. 11, pp. 14–20, 2020. **3, 6**
- [31] L. Zhang, X. Pang, S. Jia, S. Wang, and X. Yu, "Beyond 100 gb/s optoelectronic terahertz communications: Key technologies and directions," *IEEE Communications Magazine*, vol. 58, no. 11, pp. 34–40, 2020. **3, 6, 7**
- [32] M. Polese, J. M. Jornet, T. Melodia, and M. Zorzi, "Toward end-to-end, full-stack 6g terahertz networks," *IEEE Communications Magazine*, vol. 58, no. 11, pp. 48–54, 2020. **3, 6, 20, 22**
- [33] X. Huang, Y. J. Guo, and J. D. Bunton, "A hybrid adaptive antenna array," *IEEE Transactions on Wireless Communications*, vol. 9, no. 5, pp. 1770–1779, 2010. **3**
- [34] S. Diebold, S. Nakai, K. Nishio, J. Kim, K. Tsuruda, T. Mukai, M. Fujita, and T. Nagatsuma, "Modeling and simulation of terahertz resonant tunneling diode-based circuits," *IEEE Transactions on Terahertz Science and Technology*, vol. 6, no. 5, pp. 716–723, 2016. **5**
- [35] K. Kasagi, S. Suzuki, and M. Asada, "Large-scale array of resonant-tunneling-diode terahertz oscillators for high output power at 1 thz," *Journal of Applied Physics*, vol. 125, no. 15, p. 151601, 2019. **5**
- [36] A. Biswas, S. Sinha, A. Acharyya, A. Banerjee, S. Pal, H. Satoh, and H. Inokawa, "1.0 thz gap impatt source: Effect of parasitic series resistance," *Journal of Infrared, Millimeter, and Terahertz Waves*, vol. 39, no. 10, pp. 954–974, 2018. **5**
- [37] S. Banerjee, "Thz solid-state source based on impatt devices," in *Terahertz Biomedical and Healthcare Technologies*. Elsevier, 2020, pp. 1–41. **5**
- [38] A. Baig, D. Gamzina, T. Kimura, J. Atkinson, C. Domier, B. Popovic, L. Himes, R. Barchfeld, M. Field, and N. C. Luhmann, "Performance of a nano-cnc machined 220-ghz traveling wave tube amplifier," *IEEE*

- Transactions on Electron Devices*, vol. 64, no. 5, pp. 2390–2397, 2017. 5
- [39] P. Hu, W. Lei, Y. Jiang, Y. Huang, R. Song, H. Chen, and Y. Dong, “Demonstration of a watt-level traveling wave tube amplifier operating above 0.3 thz,” *IEEE Electron Device Letters*, vol. 40, no. 6, pp. 973–976, 2019. 5
- [40] S. Hara, K. Takano, K. Katayama, R. Dong, S. Lee, I. Watanabe, N. Sekine, A. Kasamatsu, T. Yoshida, S. Amakawa *et al.*, “300-ghz cmos transceiver for terahertz wireless communication,” in *Proc. of Asia-Pacific Microwave Conference (APMC)*, 2018, pp. 429–431. 6
- [41] K. Kenneth, W. Choi, Q. Zhong, N. Sharma, Y. Zhang, R. Han, Z. Ahmad, D.-Y. Kim, S. Kshattray, I. R. Medvedev *et al.*, “Opening terahertz for everyday applications,” *IEEE Communications Magazine*, vol. 57, no. 8, pp. 70–76, 2019. 6
- [42] K. M. Leong, X. Mei, W. H. Yoshida, A. Zamora, J. G. Padilla, B. S. Gorospe, K. Nguyen, and W. R. Deal, “850 ghz receiver and transmitter front-ends using inp hemt,” *IEEE Transactions on Terahertz Science and Technology*, vol. 7, no. 4, pp. 466–475, 2017. 6
- [43] J. V. Siles, K. B. Cooper, C. Lee, R. H. Lin, G. Chattopadhyay, and I. Mehdi, “A new generation of room-temperature frequency-multiplied sources with up to $10\times$ higher output power in the 160-ghz–1.6-thz range,” *IEEE Transactions on Terahertz Science and Technology*, vol. 8, no. 6, pp. 596–604, 2018. 6
- [44] A. Simsek, A. S. Ahmed, A. A. Farid, U. Soyulu, and M. J. Rodwell, “A 140ghz two-channel cmos transmitter using low-cost packaging technologies,” in *Proc. of IEEE Wireless Communications and Networking Conference Workshops (WCNC Wkps)*, 2020, pp. 1–3. 6, 8
- [45] S. Abu-Surra, W. Choi, S. Choi, E. Seok, D. Kim, N. Sharma, S. Advani, V. Loseu, K. Bae, I. Na *et al.*, “End-to-end 140 ghz wireless link demonstration with fully-digital beamformed system,” in *Proc. of IEEE International Conference on Communications Workshops (ICC Workshops)*, 2021, pp. 1–6. 6
- [46] H.-J. Song, “Packages for terahertz electronics,” *Proceedings of the IEEE*, vol. 105, no. 6, pp. 1121–1138, 2017. 6
- [47] M. Alonso-del Pino, C. Jung-Kubiak, T. Reck, C. Lee, and G. Chattopadhyay, “Micromachining for advanced terahertz: Interconnects and packaging techniques at terahertz frequencies,” *IEEE Microwave Magazine*, vol. 21, no. 1, pp. 18–34, 2019. 6
- [48] B. S. Williams, “Terahertz quantum-cascade lasers,” *Nature photonics*, vol. 1, no. 9, pp. 517–525, 2007. 7
- [49] X. Wang, C. Shen, T. Jiang, Z. Zhan, Q. Deng, W. Li, W. Wu, N. Yang, W. Chu, and S. Duan, “High-power terahertz quantum cascade lasers with 0.23 w in continuous wave mode,” *AIP Advances*, vol. 6, no. 7, p. 075210, 2016. 7
- [50] Q. Lu, F. Wang, D. Wu, S. Slivken, and M. Razeghi, “Room temperature terahertz semiconductor frequency comb,” *Nature communications*, vol. 10, no. 1, pp. 1–7, 2019. 7
- [51] A. Khalatpour, A. K. Paulsen, C. Deimert, Z. R. Wasilewski, and Q. Hu, “High-power portable terahertz laser systems,” *Nature Photonics*, vol. 15, no. 1, pp. 16–20, 2021. 7
- [52] M. Sung, S.-R. Moon, E.-S. Kim, S. Cho, J. K. Lee, S.-H. Cho, T. Kawanishi, and H.-J. Song, “Design considerations of photonic thz communications for 6g networks,” *IEEE Wireless Communications*, 2021. 7
- [53] C. C. Renaud, M. Natrella, C. Graham, J. Seddon, F. Van Dijk, and A. J. Seeds, “Antenna integrated thz uni-traveling carrier photodiodes,” *IEEE Journal of Selected Topics in Quantum Electronics*, vol. 24, no. 2, pp. 1–11, 2017. 7
- [54] N. M. Burford and M. O. El-Shenawee, “Review of terahertz photoconductive antenna technology,” *Optical Engineering*, vol. 56, no. 1, p. 010901, 2017. 7
- [55] N. T. Yardimci and M. Jarrahi, “Nanostructure-enhanced photoconductive terahertz emission and detection,” *Small*, vol. 14, no. 44, p. 1802437, 2018. 7
- [56] M. Dyakonov and M. Shur, “Shallow water analogy for a ballistic field effect transistor: New mechanism of plasma wave generation by dc current,” *Physical review letters*, vol. 71, no. 15, p. 2465, 1993. 7
- [57] W. Knap, F. Teppe, Y. Meziani, N. Dyakonova, J. Lusakowski, F. Boeuf, T. Skotnicki, D. Maude, S. Rumyantsev, and M. Shur, “Plasma wave detection of sub-terahertz and terahertz radiation by silicon field-effect transistors,” *Applied Physics Letters*, vol. 85, no. 4, pp. 675–677, 2004. 7
- [58] K. S. Novoselov, V. Fal, L. Colombo, P. Gellert, M. Schwab, K. Kim *et al.*, “A roadmap for graphene,” *Nature*, vol. 490, no. 7419, pp. 192–200, 2012. 7
- [59] J. M. Jornet and I. F. Akyildiz, “Graphene-based plasmonic nano-transceiver for terahertz band communication,” in *Proc. of European Conference on Antennas and Propagation (EuCAP)*, 2014, U.S. Patent No. 9,397,758, July 19, 2016 (Priority Date: Dec. 6, 2013). 7
- [60] J. Crabb, X. Cantos-Roman, J. M. Jornet, and G. R. Aizin, “Hydrodynamic theory of the dyakonov-shur instability in graphene transistors,” *Physical Review B*, 2021. 7
- [61] J. M. Jornet and I. F. Akyildiz, “Graphene-based nano-antennas for electromagnetic nanocommunications in the terahertz band,” in *Proc. of the Fourth European Conference on Antennas and Propagation*, 2010, pp. 1–5. 7
- [62] M. Tamagnone, J. Gomez-Diaz, J. Mosig, and J. Perruisseau-Carrier, “Analysis and design of Terahertz antennas based on plasmonic resonant graphene sheets,” *Journal of Applied Physics*, vol. 112, no. 11, p. 114915, 2012. 7
- [63] J. M. Jornet and I. F. Akyildiz, “Graphene-based plasmonic nano-antenna for terahertz band communication in nanonetworks,” *IEEE JSAC, Special Issue on Emerging Technologies for Communications*, vol. 12, no. 12, pp. 685–694, Dec. 2013, U.S. Patent No. 9,643,841, May 9, 2017 (Priority Date: Dec. 6, 2013). 7, 8
- [64] S. Abadal, I. Llatser, A. Mestres, H. Lee, E. Alarcón, and A. Cabellos-Aparicio, “Time-domain analysis of graphene-based miniaturized antennas for ultra-short-range impulse radio communications,” *IEEE Transactions on communications*, vol. 63, no. 4, pp. 1470–1482, 2015. 7
- [65] L. Vicarelli, M. Vitiello, D. Coquillat, A. Lombardo, A. C. Ferrari, W. Knap, M. Polini, V. Pellegrini, and A. Tredicucci, “Graphene field-effect transistors as room-temperature terahertz detectors,” *Nature materials*, vol. 11, no. 10, pp. 865–871, 2012. 7
- [66] D. A. Bandurin, D. Svintsov, I. Gayduchenko, S. G. Xu, A. Principi, M. Moskotin, I. Tretyakov, D. Yagodkin, S. Zhukov, T. Taniguchi *et al.*, “Resonant terahertz detection using graphene plasmons,” *Nature communications*, vol. 9, no. 1, pp. 1–8, 2018. 7
- [67] P. K. Singh, G. Aizin, N. Thawdar, M. Medley, and J. M. Jornet, “Graphene-based plasmonic phase modulator for terahertz-band communication,” in *Proc. of European Conference on Antennas and Propagation (EuCAP)*. IEEE, 2016, pp. 1–5, U.S. Patent No. 10,996,379, issued on May 4, 2021 (Priority date April 9, 2017). 7
- [68] J. Crabb, X. Cantos Roman, G. R. Aizin, and J. M. Jornet, “An on-chip amplitude and frequency modulating graphene-based plasmonic terahertz signal nano-generator,” in *Proc. of the Eight Annual ACM International Conference on Nanoscale Computing and Communication*, 2021, pp. 1–6. 7
- [69] I. F. Akyildiz and J. M. Jornet, “Electromagnetic wireless nanosensor networks,” *Nano Communication Networks*, vol. 1, no. 1, pp. 3–19, 2010. 7
- [70] I. F. Akyildiz and J. M. Jornet, “Realizing ultra-massive MIMO (1024×1024) communication in the (0.06–10) terahertz band,” *Nano Communication Networks*, vol. 8, pp. 46–54, 2016, U.S. Patent No. 9,825,712, November 21, 2017 (Priority Date: Dec. 6, 2013). 7, 8
- [71] A. Singh, M. Andreello, N. Thawdar, and J. M. Jornet, “Design and operation of a graphene-based plasmonic nano-antenna array for communication in the terahertz band,” *IEEE Journal on Selected Areas in Communications*, vol. 38, no. 9, pp. 2104–2117, 2020. 7, 8
- [72] J. Wang, H. Tian, Y. Wang, X. Li, Y. Cao, L. Li, J. Liu, and Z. Zhou, “Liquid crystal terahertz modulator with plasmon-induced transparency metamaterial,” *Optics express*, vol. 26, no. 5, pp. 5769–5776, 2018. 7
- [73] Y.-G. Jeong, Y.-M. Bahk, and D.-S. Kim, “Dynamic Terahertz Plasmonics Enabled by Phase-Change Materials,” *Advanced Optical Materials*, vol. 8, no. 3, p. 1900548, 2020. 7
- [74] K. Delfanazari, R. A. Klemm, H. J. Joyce, D. A. Ritchie, and K. Kadowaki, “Integrated, portable, tunable, and coherent terahertz sources and sensitive detectors based on layered superconductors,” *Proceedings of the IEEE*, vol. 108, no. 5, pp. 721–734, 2020. 7
- [75] K. Fan, Z.-C. Hao, Q. Yuan, and W. Hong, “Development of a high gain 325–500 ghz antenna using quasi-planar reflectors,” *IEEE Transactions on Antennas and Propagation*, vol. 65, no. 7, pp. 3384–3391, 2017. 8
- [76] VDI Passive Devices, 2019, [online] Available: <https://www.vadiodes.com/en/products/straight-waveguides-tapers-horn-antenna-directional-couplers>. 8
- [77] Mi-Wave Antennas, 2019, [online] Available: <https://www.miwave.com/millimeter-wave-products/antenna-products/>. 8
- [78] M. Esquis-Morote, J. S. Gómez-Di, J. Perruisseau-Carrier *et al.*, “Sinusoidally modulated graphene leaky-wave antenna for electronic beamscanning at thz,” *IEEE Transactions on Terahertz Science and Technology*, vol. 4, no. 1, pp. 116–122, 2014. 8
- [79] N. J. Karl, R. W. McKinney, Y. Monnai, R. Mendis, and D. M. Mittleman, “Frequency-division multiplexing in the terahertz range

- using a leaky-wave antenna," *Nature Photonics*, vol. 9, no. 11, pp. 717–720, 2015. [8](#)
- [80] K. Sengupta and A. Hajimiri, "A 0.28 thz power-generation and beam-steering array in cmos based on distributed active radiators," *IEEE Journal of Solid-State Circuits*, vol. 47, no. 12, pp. 3013–3031, 2012. [8](#)
- [81] A. Tang, N. Chahat, Y. Zhao, G. Virbila, C. Lee, F. Hsiao, L. Du, Y.-C. Kuan, M.-C. F. Chang, G. Chattopadhyay *et al.*, "A 65nm cmos 140 ghz 27.3 dbm eirp transmit array with membrane antenna for highly scalable multi-chip phase arrays," in *Proc. of IEEE MTT-S International Microwave Symposium (IMS)*, 2014, pp. 1–3. [8](#)
- [82] F. Shen, J. Qin, and Z. Han, "Planar antenna array as a highly sensitive terahertz sensor," *Applied optics*, vol. 58, no. 3, pp. 540–544, 2019. [8](#)
- [83] N. Llombart, G. Chattopadhyay, A. Skalare, and I. Mehdi, "Novel terahertz antenna based on a silicon lens fed by a leaky wave enhanced waveguide," *IEEE Transactions on Antennas and Propagation*, vol. 59, no. 6, pp. 2160–2168, 2011. [8](#)
- [84] O. Yurduseven, N. L. Juan, and A. Neto, "A dual-polarized leaky lens antenna for wideband focal plane arrays," *IEEE Transactions on Antennas and Propagation*, vol. 64, no. 8, pp. 3330–3337, 2016. [8](#)
- [85] H. Tao, A. Strikwerda, K. Fan, W. Padilla, X. Zhang, and R. Averitt, "Reconfigurable terahertz metamaterials," *Physical review letters*, vol. 103, no. 14, p. 147401, 2009. [9](#)
- [86] H. Tao, W. J. Padilla, X. Zhang, and R. D. Averitt, "Recent progress in electromagnetic metamaterial devices for terahertz applications," *IEEE Journal of Selected Topics in Quantum Electronics*, vol. 17, no. 1, pp. 92–101, 2010. [9](#)
- [87] L. Ju, B. Geng, J. Horng, C. Girit, M. Martin, Z. Hao, H. A. Bechtel, X. Liang, A. Zettl, Y. R. Shen *et al.*, "Graphene plasmonics for tunable terahertz metamaterials," *Nature nanotechnology*, vol. 6, no. 10, pp. 630–634, 2011. [9](#)
- [88] V. Pacheco-Peña, N. Engheta, S. Kuznetsov, A. Gentslev, and M. Beruete, "Experimental realization of an epsilon-near-zero graded-index metalens at terahertz frequencies," *Physical Review Applied*, vol. 8, no. 3, p. 034036, 2017. [9](#)
- [89] B. Sensale-Rodriguez, R. Yan, M. M. Kelly, T. Fang, K. Tahy, W. S. Hwang, D. Jena, L. Liu, and H. G. Xing, "Broadband graphene terahertz modulators enabled by intraband transitions," *Nature communications*, vol. 3, no. 1, pp. 1–7, 2012. [9](#)
- [90] Y. Z. Cheng, W. Withayachumnankul, A. Upadhyay, D. Headland, Y. Nie, R. Z. Gong, M. Bhaskaran, S. Sriram, and D. Abbott, "Ultrabroadband reflective polarization converter for terahertz waves," *Applied Physics Letters*, vol. 105, no. 18, p. 181111, 2014. [9](#)
- [91] S. Venkatesh, X. Lu, H. Saeidi, and K. Sengupta, "A high-speed programmable and scalable terahertz holographic metasurface based on tiled cmos chips," *Nature Electronics*, vol. 3, no. 12, pp. 785–793, 2020. [9](#)
- [92] S. Nie, J. M. Jornet, and I. F. Akyildiz, "Intelligent environments based on ultra-massive mimo platforms for wireless communication in millimeter wave and terahertz bands," in *Proc. of IEEE International Conference on Acoustics, Speech and Signal Processing (ICASSP)*, 2019, pp. 7849–7853. [9](#)
- [93] J. He, X. Wang, D. Hu, J. Ye, S. Feng, Q. Kan, and Y. Zhang, "Generation and evolution of the terahertz vortex beam," *Optics express*, vol. 21, no. 17, pp. 20230–20239, 2013. [9](#)
- [94] D. S. Dong, J. Yang, Q. Cheng, J. Zhao, L. H. Gao, S. J. Ma, S. Liu, H. B. Chen, Q. He, W. W. Liu *et al.*, "Terahertz broadband low-reflection metasurface by controlling phase distributions," *Advanced Optical Materials*, vol. 3, no. 10, pp. 1405–1410, 2015. [9](#)
- [95] L.-H. Gao, Q. Cheng, J. Yang, S.-J. Ma, J. Zhao, S. Liu, H.-B. Chen, Q. He, W.-X. Jiang, H.-F. Ma *et al.*, "Broadband diffusion of terahertz waves by multi-bit coding metasurfaces," *Light: Science & Applications*, vol. 4, no. 9, pp. e324–e324, 2015. [9](#)
- [96] E. Carrasco and J. Perruisseau-Carrier, "Reflectarray antenna at terahertz using graphene," *IEEE Antennas and Wireless Propagation Letters*, vol. 12, pp. 253–256, 2013. [9](#)
- [97] A. Singh, M. Andreello, E. Einarsson, N. Thawdar, and J. M. Jornet, "Design and operation of a smart graphene-metal hybrid reflectarray at thz frequencies," in *Proc. of IEEE European Conference on Antennas and Propagation (EuCAP)*, 2020, pp. 1–5. [9](#)
- [98] A. Singh, M. Andreello, E. Einarsson, N. Thawdar, and J. M. Jornet, "A hybrid intelligent reflecting surface with graphene-based control elements for thz communications," in *Proc. of IEEE International Workshop on Signal Processing Advances in Wireless Communications (SPAWC)*, 2020, pp. 1–5. [9](#)
- [99] C. Liaskos, S. Nie, A. Tsioliaridou, A. Pitsillides, S. Ioannidis, and I. Akyildiz, "A new wireless communication paradigm through software-controlled metasurfaces," *IEEE Communications Magazine*, vol. 56, no. 9, pp. 162–169, 2018. [9](#)
- [100] C. Liaskos, A. Tsioliaridou, A. Pitsillides, S. Ioannidis, and I. Akyildiz, "Using any surface to realize a new paradigm for wireless communications," *Communications of the ACM*, vol. 61, no. 11, pp. 30–33, 2018. [9](#)
- [101] S. Dash, G. Soni, A. Patnaik, C. Liaskos, A. Pitsillides, and I. F. Akyildiz, "Switched-beam graphene plasmonic nanoantenna in the terahertz wave region," *Plasmonics*, pp. 1–10, 2021. [9](#)
- [102] C. Han, L. Yan, and J. Yuan, "Hybrid beamforming for terahertz wireless communications: Challenges, architectures, and open problems," *IEEE Wireless Communications*, vol. 28, no. 4, pp. 198–204, 2021. [9](#), [10](#), [17](#)
- [103] S. Liu, A. Noor, L. L. Du, L. Zhang, Q. Xu, K. Luan, T. Q. Wang, Z. Tian, W. X. Tang, J. G. Han *et al.*, "Anomalous refraction and nondiffractive bessel-beam generation of terahertz waves through transmission-type coding metasurfaces," *ACS photonics*, vol. 3, no. 10, pp. 1968–1977, 2016. [9](#)
- [104] C. Liu, L. Niu, K. Wang, and J. Liu, "3d-printed diffractive elements induced accelerating terahertz airy beam," *Optics express*, vol. 24, no. 25, pp. 29342–29348, 2016. [9](#)
- [105] L. Zhu, X. Wei, J. Wang, Z. Zhang, Z. Li, H. Zhang, S. Li, K. Wang, and J. Liu, "Experimental demonstration of basic functionalities for 0.1-thz orbital angular momentum (oam) communications," in *Proc. of IEEE OFC*, 2014, pp. 1–3. [9](#)
- [106] X. Su, R. Zhang, Z. Zhao, H. Song, A. Minoofar, N. Hu, H. Zhou, K. Zou, K. Pang, H. Song *et al.*, "Multipath and receiver aperture effects in a thz wireless communications link using oam multiplexing," in *Proc. of IEEE Globecom Workshops*, 2020, pp. 1–6. [9](#)
- [107] Y. Xie, Z. Geng, L. Zhuang, M. Burla, C. Taddei, M. Hoekman, A. Leinse, C. G. Roeloffzen, K.-J. Boller, and A. J. Lowery, "Programmable optical processor chips: toward photonic rf filters with dsp-level flexibility and mhz-band selectivity," *Nanophotonics*, vol. 7, no. 2, pp. 421–454, 2018. [9](#)
- [108] R. Tang, R. Tanomura, T. Tanemura, and Y. Nakano, "Ten-port unitary optical processor on a silicon photonic chip," *ACS Photonics*, 2021. [9](#)
- [109] Y. Fu, X. Hu, C. Lu, S. Yue, H. Yang, and Q. Gong, "All-optical logic gates based on nanoscale plasmonic slot waveguides," *Nano letters*, vol. 12, no. 11, pp. 5784–5790, 2012. [9](#)
- [110] N. Gogoi and P. P. Sahu, "All-optical surface plasmonic universal logic gate devices," *Plasmonics*, vol. 11, no. 6, pp. 1537–1542, 2016. [9](#)
- [111] M. Nagatani, H. Wakita, T. Jyo, M. Mutoh, M. Ida, S. P. Voinigescu, and H. Nosaka, "A 256-gbps pam-4 signal generator ic in 0.25- μ m inp dbbt technology," in *Proc. of IEEE BiCMOS and Compound Semiconductor Integrated Circuits and Technology Symposium (BCICTS)*, 2018, pp. 28–31. [9](#)
- [112] A. Buchwald, "High-speed time interleaved adcs," *IEEE Communications Magazine*, vol. 54, no. 4, pp. 71–77, 2016. [9](#)
- [113] C. Han, A. O. Bicen, and I. F. Akyildiz, "Multi-ray channel modeling and wideband characterization for wireless communications in the terahertz band," *IEEE Transactions on Wireless Communications*, vol. 14, no. 5, pp. 2402–2412, 2015. [10](#)
- [114] V. Ariyaratna, A. Madanayake, and J. M. Jornet, "Real-time digital baseband system for ultra-broadband thz communication," in *Proc. of International Conference on Infrared, Millimeter, and Terahertz Waves (IRMMW-THz)*, 2020, pp. 1–2. [10](#)
- [115] I. Mehdi, "THz instruments for space exploration," in *IEEE Asia Pacific Microwave Conference (APMC)*, 2017, pp. 410–413. [10](#)
- [116] J. M. Jornet and I. F. Akyildiz, "Channel Modeling and Capacity Analysis of Electromagnetic Wireless Nanonetworks in the Terahertz Band," *IEEE Transactions on Wireless Communications*, vol. 10, no. 10, pp. 3211–3221, Oct. 2011. [10](#)
- [117] C. Han, A. O. Bicen, and I. F. Akyildiz, "Multi-Ray Channel Modeling and Wideband Characterization for Wireless Communications in the Terahertz Band," *IEEE Transactions on Wireless Communications*, vol. 14, no. 5, pp. 2402–2412, 2015. [10](#), [12](#), [13](#)
- [118] S. Priebe and T. Kurner, "Stochastic modeling of thz indoor radio channels," *IEEE Transactions on Wireless Communications*, vol. 12, no. 9, pp. 4445–4455, 2013. [10](#), [12](#)
- [119] Y. Chen, Y. Li, C. Han, Z. Yu, and G. Wang, "Channel measurement and ray-tracing-statistical hybrid modeling for low-terahertz indoor communications," *IEEE Transactions on Wireless Communications*, pp. 1–1, 2021. [10](#), [12](#)
- [120] S. Ju, Y. Xing, O. Kanhere, and T. S. Rappaport, "Millimeter wave and sub-terahertz spatial statistical channel model for an indoor office building," *IEEE Journal on Selected Areas in Communications*, vol. 39, no. 6, pp. 1561–1575, 2021. [10](#)

- [121] N. A. Abbasi, J. Gomez-Ponce, S. M. Shaikbepari, S. Rao, R. Kondaveti, S. Abu-Surra, G. Xu, C. Zhang, and A. F. Molisch, "Ultra-wideband double directional channel measurements for thz communications in urban environments," in *ICC 2021-IEEE International Conference on Communications*, 2021, pp. 1–6. [10](#)
- [122] A. W. Mbugua, W. Fan, K. Olesen, X. Cai, and G. F. Pedersen, "Phase-compensated optical fiber-based ultrawideband channel sounder," *IEEE Transactions on Microwave Theory and Techniques*, vol. 68, no. 2, pp. 636–647, 2020. [10](#)
- [123] Z. Yu, Y. Chen, G. Wang, W. Gao, and C. Han, "Wideband channel measurements and temporal-spatial analysis for terahertz indoor communications," in *Proc. of IEEE International Conference on Communications Workshops (ICC Workshops)*, 2020, pp. 1–6. [11](#)
- [124] J. He, Y. Chen, Y. Wang, Z. Yu, and C. Han, "Wideband channel measurements and temporal-spatial analysis for terahertz indoor communications," in *Proc. of IEEE International Conference on Communications Workshops (ICC Workshops)*, 2021, pp. 1–6. [11](#)
- [125] N. A. Abbasi, A. Hariharan, A. M. Nair, A. S. Almaini, F. B. Rotenberg, A. E. Willner, and A. F. Molisch, "Double directional channel measurements for thz communications in an urban environment," in *Proc. of IEEE International Conference on Communications (ICC)*, 2020, pp. 1–6. [11](#)
- [126] N. A. Abbasi, A. Hariharan, A. M. Nair, and A. F. Molisch, "Channel measurements and path loss modeling for indoor thz communication," in *Proc. of European Conference on Antennas and Propagation (EuCAP)*, 2020, pp. 1–5. [11](#)
- [127] S. Kim and A. G. Zajić, "Statistical characterization of 300-ghz propagation on a desktop," *IEEE Transactions on Vehicular Technology*, vol. 64, no. 8, pp. 3330–3338, 2015. [11](#)
- [128] S. Kim and A. Zajić, "Characterization of 300-ghz wireless channel on a computer motherboard," *IEEE Transactions on Antennas and Propagation*, vol. 64, no. 12, pp. 5411–5423, 2016. [11](#)
- [129] C.-L. Cheng and A. Zajić, "Characterization of propagation phenomena relevant for 300 ghz wireless data center links," *IEEE Transactions on Antennas and Propagation*, vol. 68, no. 2, pp. 1074–1087, 2020. [11](#)
- [130] H. Cox, "Spatial correlation in arbitrary noise fields with application to ambient sea noise," *The Journal of the Acoustical Society of America*, vol. 54, no. 5, pp. 1289–1301, 1973. [11](#)
- [131] G. R. MacCartney and T. S. Rappaport, "A flexible millimeter-wave channel sounder with absolute timing," *IEEE Journal on Selected Areas in Communications*, vol. 35, no. 6, pp. 1402–1418, 2017. [11](#)
- [132] S. Ju, S. H. A. Shah, M. A. Javed, J. Li, G. Palteru, J. Robin, Y. Xing, O. Kanhere, and T. S. Rappaport, "Scattering mechanisms and modeling for terahertz wireless communications," in *Proc. of IEEE International Conference on Communications (ICC)*, 2019, pp. 1–7. [11](#)
- [133] Y. Xing and T. S. Rappaport, "Propagation measurement system and approach at 140 ghz-moving to 6g and above 100 ghz," in *Proc. of IEEE Global Communications Conference (GLOBECOM)*, 2018, pp. 1–6. [11](#)
- [134] Y. Xing and T. S. Rappaport, "Terahertz wireless communications: Co-sharing for terrestrial and satellite systems above 100 ghz," *IEEE Communications Letters*, pp. 1–1, 2021. [11, 15](#)
- [135] S. Rey, J. M. Eckhardt, B. Peng, K. Guan, and T. Kürner, "Channel sounding techniques for applications in thz communications: A first correlation based channel sounder for ultra-wideband dynamic channel measurements at 300 ghz," in *International Congress on Ultra Modern Telecommunications and Control Systems and Workshops (ICUMT)*, 2017, pp. 449–453. [11](#)
- [136] K. Guan, G. Li, T. Kürner, A. F. Molisch, B. Peng, R. He, B. Hui, J. Kim, and Z. Zhong, "On millimeter wave and thz mobile radio channel for smart rail mobility," *IEEE Transactions on Vehicular Technology*, vol. 66, no. 7, pp. 5658–5674, 2017. [11](#)
- [137] K. Guan, D. He, B. Ai, Y. Chen, C. Han, B. Peng, Z. Zhong, and T. Kürner, "Channel characterization and capacity analysis for thz communication enabled smart rail mobility," *IEEE Transactions on Vehicular Technology*, vol. 70, no. 5, pp. 4065–4080, 2021. [11](#)
- [138] K. Guan, B. Peng, D. He, J. M. Eckhardt, S. Rey, B. Ai, Z. Zhong, and T. Kürner, "Measurement, simulation, and characterization of train-to-infrastructure inside-station channel at the terahertz band," *IEEE Transactions on Terahertz Science and Technology*, vol. 9, no. 3, pp. 291–306, 2019. [11](#)
- [139] K. Guan, B. Peng, D. He, J. M. Eckhardt, S. Rey, B. Ai, Z. Zhong, and T. Kürner, "Channel characterization for intra-wagon communication at 60 and 300 ghz bands," *IEEE Transactions on Vehicular Technology*, vol. 68, no. 6, pp. 5193–5207, 2019. [11](#)
- [140] J. M. Eckhardt, V. Petrov, D. Moltchanov, Y. Koucheryavy, and T. Kürner, "Channel measurements and modeling for low-terahertz band vehicular communications," *IEEE Journal on Selected Areas in Communications*, vol. 39, no. 6, pp. 1590–1603, 2021. [11, 15](#)
- [141] J. M. Eckhardt, T. Doeker, and T. Kürner, "Indoor-to-outdoor path loss measurements in an aircraft for terahertz communications," in *Proc. of IEEE Vehicular Technology Conference (VTC2020-Spring)*, 2020, pp. 1–5. [11](#)
- [142] H. Harde, R. Cheville, and D. Grischkowsky, "Terahertz studies of collision-broadened rotational lines," *The Journal of Physical Chemistry A*, vol. 101, no. 20, pp. 3646–3660, 1997. [11](#)
- [143] Z. Hossain, C. N. Mollica, J. F. Federici, and J. M. Jornet, "Stochastic interference modeling and experimental validation for pulse-based terahertz communication," *IEEE Transactions on Wireless Communications*, vol. 18, no. 8, pp. 4103–4115, 2019. [11](#)
- [144] R. Piesiewicz, C. Jansen, D. Mittleman, T. Kleine-Ostmann, M. Koch, and T. Kurner, "Scattering analysis for the modeling of thz communication systems," *IEEE Transactions on Antennas and Propagation*, vol. 55, no. 11, pp. 3002–3009, 2007. [11](#)
- [145] C. Jansen, R. Piesiewicz, D. Mittleman, T. Kurner, and M. Koch, "The impact of reflections from stratified building materials on the wave propagation in future indoor terahertz communication systems," *IEEE Transactions on Antennas and Propagation*, vol. 56, no. 5, pp. 1413–1419, 2008. [11](#)
- [146] C. Jansen, S. Priebe, C. Moller, M. Jacob, H. Dierke, M. Koch, and T. Kurner, "Diffuse scattering from rough surfaces in thz communication channels," *IEEE Transactions on Terahertz Science and Technology*, vol. 1, no. 2, pp. 462–472, 2011. [11](#)
- [147] J. M. Jornet and I. F. Akyildiz, "Channel modeling and capacity analysis for electromagnetic wireless nanonetworks in the terahertz band," *IEEE Transactions on Wireless Communications*, vol. 10, no. 10, pp. 3211–3221, 2011. [11](#)
- [148] J. S. Lu, E. M. Vitucci, V. Degli-Esposti, F. Fuschini, M. Barbiroli, J. A. Blaha, and H. L. Bertoni, "A discrete environment-driven gpu-based ray launching algorithm," *IEEE Transactions on Antennas and Propagation*, vol. 67, no. 2, pp. 1180–1192, 2019. [12](#)
- [149] S. Priebe, M. Kannicht, M. Jacob, and T. Kürner, "Ultra broadband indoor channel measurements and calibrated ray tracing propagation modeling at thz frequencies," *Journal of Communications and Networks*, vol. 15, no. 6, pp. 547–558, 2013. [12](#)
- [150] C. Han and I. F. Akyildiz, "Three-Dimensional End-to-End Modeling and Analysis for Graphene-Enabled Terahertz Band Communications," *IEEE Transactions on Vehicular Technology*, pp. 313–316, 2017. [12, 13](#)
- [151] S. Nie and I. F. Akyildiz, "Three-Dimensional Dynamic Channel Modeling and Tracking for Terahertz Band Indoor Communications," *IEEE International Symposium on Personal, Indoor and Mobile Radio Communications (PIMRC)*, October 2017. [12](#)
- [152] Y. Zhao, Y. Hao, and C. Parini, "Fdd characterization of uwb indoor radio channel including frequency dependent antenna directivities," *IEEE Antennas and Wireless Propagation Letters*, vol. 6, pp. 191–194, 2007. [12](#)
- [153] M. R. Akdeniz, Y. Liu, M. K. Samimi, S. Sun, S. Rangan, T. S. Rappaport, and E. Erkip, "Millimeter wave channel modeling and cellular capacity evaluation," *IEEE Journal on Selected Areas in Communications*, vol. 32, no. 6, pp. 1164–1179, 2014. [12](#)
- [154] L. You, X. Gao, G. Y. Li, X.-G. Xia, and N. Ma, "Bdma for millimeter-wave/terahertz massive mimo transmission with per-beam synchronization," *IEEE Journal on Selected Areas in Communications*, vol. 35, no. 7, pp. 1550–1563, 2017. [12, 18](#)
- [155] Y. Wang, S. Safavi-Naeini, and S. Chaudhuri, "A hybrid technique based on combining ray tracing and fdd methods for site-specific modeling of indoor radio wave propagation," *IEEE Transactions on Antennas and Propagation*, vol. 48, no. 5, pp. 743–754, 2000. [12](#)
- [156] M. Thiel and K. Sarabandi, "A hybrid method for indoor wave propagation modeling," *IEEE Transactions on Antennas and Propagation*, vol. 56, no. 8, pp. 2703–2709, 2008. [12](#)
- [157] Y. Choi, J.-W. Choi, and J. M. Cioffi, "A geometric-statistic channel model for thz indoor communications," *Journal of Infrared, Millimeter, and Terahertz Waves*, vol. 34, no. 7–8, pp. 456–467, 2013. [12](#)
- [158] Z. Huang and X. Cheng, "A general 3d space-time-frequency non-stationary model for 6g channels," *IEEE Transactions on Wireless Communications*, vol. 20, no. 1, pp. 535–548, 2021. [12](#)
- [159] C. Chaccour, M. N. Soorki, W. Saad, M. Bennis, P. Popovski, and M. Debbah, "Seven defining features of terahertz (thz) wireless systems: A fellowship of communication and sensing," *arXiv preprint arXiv:2102.07668*, 2021. [13](#)
- [160] C. Han and I. F. Akyildiz, "Distance-aware bandwidth-adaptive resource allocation for wireless systems in the Terahertz band," *IEEE*

- Transactions on Terahertz Science and Technology*, vol. 6, no. 4, pp. 541–553, 2016. 13, 20
- [161] Y. Chen and C. Han, “Time-varying channel modeling for low-terahertz urban vehicle-to-infrastructure communications,” in *Proc. of IEEE Global Communications Conference (GLOBECOM)*, 2019, pp. 1–6. 13
- [162] C. Han, J. M. Jornet, and I. Akyildiz, “Ultra-massive mimo channel modeling for graphene-enabled terahertz-band communications,” in *Proc. of IEEE Vehicular Technology Conference (VTC Spring)*, 2018, pp. 1–5. 13
- [163] K. Rikkinen, P. Kyosti, M. E. Leinonen, M. Berg, and A. Parssinen, “Thz radio communication: Link budget analysis toward 6g,” *IEEE Communications Magazine*, vol. 58, no. 11, pp. 22–27, 2020. 14
- [164] A.-A. A. Boulogeorgos, J. M. Jornet, and A. Alexiou, “A quantitative look at directional terahertz communication systems for 6g: Fact check,” in *to appear in IEEE Vehicular Technology Magazine*. 14
- [165] J. Kokkonen, J. M. Jornet, V. Petrov, Y. Koucheryav, and M. Juntti, “Channel modeling and performance analysis of airplane-satellite terahertz band communications,” *IEEE Transactions on Vehicular Technology*, vol. 70, no. 3, pp. 2047–2061, 2021. 15
- [166] S. Nie and I. F. Akyildiz, “Channel Modeling and Analysis of Inter-Small-Satellite Links in Terahertz Band Space Networks,” *IEEE Transactions on Communications*, vol. 69, no. 12, pp. 8585–8599, 2021. 15
- [167] J. M. Jornet and I. F. Akyildiz, “Information capacity of pulse-based wireless nanosensor networks,” in *Proc. of IEEE Communications Society Conference on Sensor, Mesh and Ad Hoc Communications and Networks*, 2011, pp. 80–88. 16
- [168] J. M. Jornet and I. F. Akyildiz, “Femtosecond-long pulse-based modulation for terahertz band communication in nanonetworks,” *IEEE Transactions on Communications*, vol. 62, no. 5, pp. 1742–1754, 2014. 16
- [169] T. Mao and Z. Wang, “Terahertz wireless communications with flexible index modulation aided pilot design,” *IEEE Journal on Selected Areas in Communications*, vol. 39, no. 6, pp. 1651–1662, 2021. 16
- [170] C. Han, A. O. Bicen, and I. F. Akyildiz, “Multi-Wideband Waveform Design for Distance-adaptive Wireless Communications in the Terahertz Band,” *IEEE Transactions on Signal Processing*, no. 4, pp. 901–922, 2016. 16
- [171] Z. Hossain and J. M. Jornet, “Hierarchical bandwidth modulation for ultra-broadband terahertz communications,” in *Proc. of IEEE International Conference on Communications (ICC)*. IEEE, 2019, pp. 1–7. 16
- [172] H. Jiang and P. A. Wilford, “A hierarchical modulation for upgrading digital broadcast systems,” *IEEE Transactions on Broadcasting*, vol. 51, no. 2, pp. 223–229, 2005. 16
- [173] Y. Wu, F. Lemic, C. Han, and Z. Chen, “A non-uniform multi-wideband ofdm system for terahertz joint communication and sensing,” in *Proc. of IEEE Vehicular Technology Conference (VTC2021-Spring)*, 2021, pp. 1–5. 16
- [174] Y. Wu, F. Lemic, C. Han, and Z. Chen, “A sensing integrated dft-spread ofdm system for terahertz communications,” in *Proc. of IEEE Vehicular Technology Conference (VTC2021-Spring)*, 2021, pp. 1–5. 16
- [175] Z. Wei, W. Yuan, S. Li, J. Yuan, G. Bharatula, R. Hadani, and L. Hanzo, “Orthogonal time-frequency space modulation: A promising next-generation waveform,” *IEEE Wireless Communications*, vol. 28, no. 4, pp. 136–144, 2021. 16
- [176] Y. Wu, C. Han, and T. Yang, “Dft-spread orthogonal time frequency space modulation design for terahertz communications,” in *Proc. of IEEE Globecom*, 2021. 16
- [177] J. M. Jornet, “Low-weight error-prevention codes for electromagnetic nanonetworks in the terahertz band,” *Nano Communication Networks*, vol. 5, no. 1–2, pp. 35–44, 2014. 16
- [178] X.-W. Yao, D.-B. Ma, and C. Han, “Ecp: A probing-based error control strategy for thz-based nanonetworks with energy harvesting,” *IEEE Access*, vol. 7, pp. 25 616–25 626, 2019. 16
- [179] B. Peng, S. Wesemann, K. Guan, W. Templ, and T. Kürner, “Precoding and detection for broadband single carrier terahertz massive mimo systems using lsqr algorithm,” *IEEE Transactions on Wireless Communications*, vol. 18, no. 2, pp. 1026–1040, 2019. 17
- [180] H. Yuan, N. Yang, K. Yang, C. Han, and J. An, “Hybrid beamforming for terahertz multi-carrier systems over frequency selective fading,” *IEEE Transactions on Communications*, vol. 68, no. 10, pp. 6186–6199, 2020. 17
- [181] F. Gao, B. Wang, C. Xing, J. An, and G. Y. Li, “Wideband beamforming for hybrid massive mimo terahertz communications,” *IEEE Journal on Selected Areas in Communications*, vol. 39, no. 6, pp. 1725–1740, 2021. 17
- [182] Q. Wan, J. Fang, Z. Chen, and H. Li, “Hybrid precoding and combining for millimeter wave/sub-thz mimo-ofdm systems with beam squint effects,” *IEEE Transactions on Vehicular Technology*, vol. 70, no. 8, pp. 8314–8319, 2021. 17
- [183] W. Hao, G. Sun, M. Zeng, Z. Chu, Z. Zhu, O. A. Dobre, and P. Xiao, “Robust design for intelligent reflecting surface-assisted mimo-ofdma terahertz iot networks,” *IEEE Internet of Things Journal*, vol. 8, no. 16, pp. 13 052–13 064, 2021. 17
- [184] B. Ning, Z. Chen, W. Chen, Y. Du, and J. Fang, “Terahertz multi-user massive mimo with intelligent reflecting surface: Beam training and hybrid beamforming,” *IEEE Transactions on Vehicular Technology*, vol. 70, no. 2, pp. 1376–1393, 2021. 17
- [185] L. Yan, C. Han, and J. Yuan, “A dynamic array-of-subarrays architecture and hybrid precoding algorithms for terahertz wireless communications,” *IEEE Journal on Selected Areas in Communications*, vol. 38, no. 9, pp. 2041–2056, 2020. 17
- [186] S. A. Busari, K. M. S. Huq, S. Mumtaz, J. Rodriguez, Y. Fang, D. C. Sicker, S. Al-Rubaye, and A. Tsourdos, “Generalized hybrid beamforming for vehicular connectivity using thz massive mimo,” *IEEE Transactions on Vehicular Technology*, vol. 68, no. 9, pp. 8372–8383, 2019. 17
- [187] L. Yan, C. Han, N. Yang, and J. Yuan, “Dynamic-subarray with quantized- and fixed-phase shifters for terahertz hybrid beamforming,” in *Proc. of IEEE Global Communications Conference*, 2020, pp. 1–6. 17
- [188] J. Tan and L. Dai, “Delay-phase precoding for thz massive mimo with beam split,” in *Proc. of IEEE Global Communications Conference (GLOBECOM)*, 2019, pp. 1–6. 17
- [189] L. Yan, C. Han, and J. Yuan, “Energy-efficient Dynamic-subarray with Fixed True-time-delay Design for Terahertz Wideband Hybrid Beamforming,” *to appear in IEEE Journal on Selected Areas in Communications (JSAC)*, 2022. 17
- [190] A. Alkhateeb, O. El Ayach, G. Leus, and R. W. Heath, “Channel estimation and hybrid precoding for millimeter wave cellular systems,” *IEEE journal of selected topics in signal processing*, vol. 8, no. 5, pp. 831–846, 2014. 17
- [191] C. Lin, G. Y. Li, and L. Wang, “Subarray-based coordinated beamforming training for mmwave and sub-thz communications,” *IEEE Journal on Selected Areas in Communications*, vol. 35, no. 9, pp. 2115–2126, 2017. 17
- [192] Y. Chen, L. Yan, and C. Han, “Millidegree-level direction-of-arrival (doa) estimation and tracking for terahertz wireless communications,” in *Proc. of IEEE International Conference on Sensing, Communication, and Networking (SECON)*, 2020, pp. 1–9. 17
- [193] X. Ma, Z. Chen, W. Chen, Z. Li, Y. Chi, C. Han, and S. Li, “Joint channel estimation and data rate maximization for intelligent reflecting surface assisted terahertz mimo communication systems,” *IEEE Access*, vol. 8, pp. 99 565–99 581, 2020. 18
- [194] K. Dovelos, M. Matthaiou, H. Q. Ngo, and B. Bellalta, “Channel estimation and hybrid combining for wideband terahertz massive mimo systems,” *IEEE Journal on Selected Areas in Communications*, vol. 39, no. 6, pp. 1604–1620, 2021. 18
- [195] A. Liao, Z. Gao, D. Wang, H. Wang, H. Yin, D. W. K. Ng, and M.-S. Alouini, “Terahertz ultra-massive mimo-based aeronautical communications in space-air-ground integrated networks,” *IEEE Journal on Selected Areas in Communications*, vol. 39, no. 6, pp. 1741–1767, 2021. 18
- [196] B. Zhai, Y. Zhu, A. Tang, and X. Wang, “Thzprism: Frequency-based beam spreading for terahertz communication systems,” *IEEE Wireless Communications Letters*, vol. 9, no. 6, pp. 897–900, 2020. 18
- [197] B. Zhai, A. Tang, C. Peng, and X. Wang, “Ss-ofdma: Spatial-spread orthogonal frequency division multiple access for terahertz networks,” *IEEE Journal on Selected Areas in Communications*, vol. 39, no. 6, pp. 1678–1692, 2021. 18
- [198] J. Tan and L. Dai, “Wideband beam tracking in thz massive mimo systems,” *IEEE Journal on Selected Areas in Communications*, vol. 39, no. 6, pp. 1693–1710, 2021. 18
- [199] Y. Chen and C. Han, “Deep cnn-based spherical-wave channel estimation for terahertz ultra-massive mimo systems,” in *Proc. of IEEE Global Communications Conference*, 2020, pp. 1–6. 18
- [200] Y. Chen, L. Yan, C. Han, and M. Tao, “Millidegree-level direction-of-arrival estimation and tracking for terahertz ultra-massive mimo systems,” *IEEE Transactions on Wireless Communications*, pp. 1–1, 2021. 18
- [201] A. Gupta, M. Medley, and J. M. Jornet, “Joint synchronization and symbol detection design for pulse-based communications in the thz

- band," in *Proc. IEEE Global Communications Conference (GLOBE-COM)*, 2015, pp. 1–7. [18](#)
- [202] Q. Xia, Z. Hossain, M. Medley, and J. M. Jornet, "A link-layer synchronization and medium access control protocol for terahertz-band communication networks," *IEEE Transactions on Mobile Computing*, vol. 20, no. 1, pp. 2–18, 2021. [18](#), [20](#)
- [203] C. Han, I. F. Akyildiz, and W. H. Gerstacker, "Timing Acquisition and Error Analysis for Pulse-Based Terahertz Band Wireless Systems," *IEEE Transactions on Vehicular Technology*, vol. 66, no. 11, pp. 10 102–10 113, 2017. [18](#)
- [204] Z. Chen, C. Han, Y. Wu, L. Li, C. Huang, Z. Zhang, G. Wang, and W. Tong, "Terahertz wireless communications for 2030 and beyond: A cutting-edge frontier," to appear in *IEEE Communications Magazine*, 2021. [18](#), [19](#), [21](#)
- [205] H. Saeed, N. Saeed, T. Y. Al-Naffouri, and M.-S. Alouini, "Next generation terahertz communications: A rendezvous of sensing, imaging, and localization," *IEEE Communications Magazine*, vol. 58, no. 5, pp. 69–75, 2020. [18](#)
- [206] M. El-Absi, A. A.-H. Abbas, A. Abuelhaija, K. Solbach, and T. Kaiser, "Distance and tag aware localization in indoor terahertz systems," in *Proc. of First International Workshop on Mobile Terahertz Systems (IWMTS)*. IEEE, 2018, pp. 1–5. [18](#)
- [207] M. El-Absi, A. A.-H. Abbas, A. Abuelhaija, F. Zheng, K. Solbach, and T. Kaiser, "High-accuracy indoor localization based on chipless rfid systems at thz band," *IEEE access*, vol. 6, pp. 54 355–54 368, 2018. [18](#)
- [208] J. Simonjan, B. D. Unluturk, and I. F. Akyildiz, "In-body bionanosensor localization for anomaly detection via inertial positioning and thz backscattering communication," to appear in *IEEE Transactions on NanoBioscience*, 2021. [18](#)
- [209] G. Stratakis, A.-A. A. Boulogeorgos, and A. Alexiou, "A cooperative localization-aided tracking algorithm for thz wireless systems," in *Proc. of IEEE Wireless Communications and Networking Conference (WCNC)*, 2019, pp. 1–7. [18](#)
- [210] S. Fan, Y. Wu, C. Han, and X. Wang, "A structured bidirectional lstm deep learning method for 3d terahertz indoor localization," in *Proc. of IEEE INFOCOM*, 2020, pp. 2381–2390. [18](#)
- [211] S. Fan, Y. Wu, C. Han, and X. Wang, "Siabr: A structured intra-attention bidirectional recurrent deep learning method for ultra-accurate terahertz indoor localization," *IEEE Journal on Selected Areas in Communications*, vol. 39, no. 7, pp. 2226–2240, 2021. [18](#)
- [212] J. Ma, R. Shrestha, J. Adelberg, C.-Y. Yeh, Z. Hossain, E. Knightly, J. M. Jornet, and D. M. Mittleman, "Security and eavesdropping in terahertz wireless links," *Nature*, vol. 563, no. 7729, pp. 89–93, 2018. [18](#), [19](#)
- [213] W. Gao, C. Han, and Z. Chen, "Receiver artificial noise aided terahertz secure communications with eavesdropper in close proximity," in *GLOBECOM 2020 - 2020 IEEE Global Communications Conference*, 2020, pp. 1–6. [18](#)
- [214] W. Gao, Y. Chen, C. Han, and Z. Chen, "Distance-adaptive absorption-peak hopping (da-aph) modulation for terahertz covert communications," in *2019 IEEE Global Communications Conference (GLOBE-COM)*, 2019, pp. 1–6. [18](#)
- [215] V. Petrov, D. Moltchanov, J. M. Jornet, and Y. Koucheryavy, "Exploiting multipath terahertz communications for physical layer security in beyond 5g networks," in *Proc. of IEEE Conference on Computer Communications Workshops (INFOCOM WKSHPS)*, 2019, pp. 865–872. [19](#)
- [216] Z. Liu, J. Liu, Y. Zeng, and J. Ma, "Covert wireless communication in iot network: From awgn channel to thz band," *IEEE Internet of Things Journal*, vol. 7, no. 4, pp. 3378–3388, 2020. [19](#)
- [217] W. Gao, Y. Chen, C. Han, and Z. Chen, "Distance-adaptive absorption peak modulation (da-aph) for terahertz covert communications," *IEEE Transactions on Wireless Communications*, vol. 20, no. 3, pp. 2064–2077, 2021. [19](#)
- [218] W. Gao, C. Han, and Z. Chen, "Dnn-powered sic-free receiver artificial noise aided terahertz secure communications with randomly distributed eavesdroppers," *IEEE Transactions on Wireless Communications*, 2021. [19](#)
- [219] X. Song, W. Rave, N. Babu, S. Majhi, and G. Fettweis, "Two-level spatial multiplexing using hybrid beamforming for millimeter-wave backhaul," *IEEE Transactions on Wireless Communications*, vol. 17, no. 7, pp. 4830–4844, 2018. [19](#)
- [220] L. Yan, C. Han, and J. Yuan, "Joint inter-and-intra-multiplexing and hybrid beamforming for terahertz widely-spaced multi-subarray systems," to appear in *IEEE Transactions on Communications*, 2022. [19](#)
- [221] H. Do, S. Cho, J. Park, H.-J. Song, N. Lee, and A. Lozano, "Terahertz line-of-sight mimo communication: Theory and practical challenges," *IEEE Communications Magazine*, vol. 59, no. 3, pp. 104–109, 2021. [19](#)
- [222] Z. Chen, C. Han, B. Ning, Z. Tian, and S. Li, "Intelligent reflecting surfaces assisted terahertz communications toward 6g," *IEEE Wireless Communications*, to appear, 2021. [19](#)
- [223] Z. Wan, Z. Gao, F. Gao, M. D. Renzo, and M.-S. Alouini, "Terahertz massive mimo with holographic reconfigurable intelligent surfaces," *IEEE Transactions on Communications*, vol. 69, no. 7, pp. 4732–4750, 2021. [19](#)
- [224] A.-A. A. Boulogeorgos and A. Alexiou, "Coverage analysis of reconfigurable intelligent surface assisted thz wireless systems," *IEEE Open Journal of Vehicular Technology*, vol. 2, pp. 94–110, 2021. [19](#)
- [225] C. Han, X. Zhang, and X. Wang, "On medium access control schemes for wireless networks in the millimeter-wave and terahertz bands," *Nano Communication Networks*, vol. 19, pp. 67–80, 2019. [20](#)
- [226] S. Ghafoor, N. Boujnah, M. H. Rehmani, and A. Davy, "Mac protocols for terahertz communication: A comprehensive survey," *IEEE Communications Surveys Tutorials*, vol. 22, no. 4, pp. 2236–2282, 2020. [20](#)
- [227] Y. Ghasempour, R. Shrestha, A. Charous, E. Knightly, and D. M. Mittleman, "Single-shot link discovery for terahertz wireless networks," *Nature communications*, vol. 11, no. 1, pp. 1–6, 2020. [20](#)
- [228] Q. Xia and J. M. Jornet, "Expedited neighbor discovery in directional terahertz communication networks enhanced by antenna side-lobe information," *IEEE Transactions on Vehicular Technology*, vol. 68, no. 8, pp. 7804–7814, 2019. [20](#)
- [229] X.-W. Yao and J. M. Jornet, "Tab-mac: Assisted beamforming mac protocol for terahertz communication networks," *Elsevier Nano Communication Networks*, vol. 9, pp. 36–42, 2016. [20](#)
- [230] X. Zhang, C. Han, and X. Wang, "Dual-radio-assisted (dra) mac protocols for distributed terahertz networks," *IEEE Open Journal of Vehicular Technology*, vol. 2, pp. 111–124, 2021. [20](#)
- [231] A. S. Cacciapuoti, K. Sankhe, M. Caleffi, and K. R. Chowdhury, "Beyond 5g: Thz-based medium access protocol for mobile heterogeneous networks," *IEEE Communications Magazine*, vol. 56, no. 6, pp. 110–115, 2018. [20](#)
- [232] X. Zhang, C. Han, and X. Wang, "Joint beamforming-power-bandwidth allocation in terahertz noma networks," in *Proc. of IEEE SECON*, 2019, pp. 1–9. [20](#)
- [233] H. Zhang, H. Zhang, W. Liu, K. Long, J. Dong, and V. C. M. Leung, "Energy efficient user clustering, hybrid precoding and power optimization in terahertz mimo-noma systems," *IEEE Journal on Selected Areas in Communications*, vol. 38, no. 9, pp. 2074–2085, 2020. [20](#)
- [234] H. Zhang, Y. Duan, K. Long, and V. C. M. Leung, "Energy efficient resource allocation in terahertz downlink noma systems," *IEEE Transactions on Communications*, vol. 69, no. 2, pp. 1375–1384, 2021. [20](#)
- [235] C. Han and I. F. Akyildiz, "Distance-Aware Multi-Carrier (DAMC) Modulation in Terahertz Band Communication," in *Proc. of IEEE International Conference on Communications (ICC)*, June 2014. [20](#)
- [236] A. Shafie, N. Yang, S. Alvi, C. Han, S. Durrani, and J. Jornet, "Spectrum Allocation with Adaptive Sub-band Bandwidth for Terahertz Communication Systems," to appear in *IEEE Transactions on Communications*, 2022. [20](#)
- [237] V. Petrov, M. Komarov, D. Moltchanov, J. M. Jornet, and Y. Koucheryavy, "Interference and sinr in millimeter wave and terahertz communication systems with blocking and directional antennas," *IEEE Transactions on Wireless Communications*, vol. 16, no. 3, pp. 1791–1808, 2017. [20](#)
- [238] Y. Wu, J. Kokkonen, C. Han, and M. Juntti, "Interference and coverage analysis for terahertz networks with indoor blockage effects and line-of-sight access point association," *IEEE Transactions on Wireless Communications*, vol. 20, no. 3, pp. 1472–1486, 2021. [20](#), [21](#)
- [239] A. Shafie, N. Yang, S. Durrani, X. Zhou, C. Han, and M. Juntti, "Coverage analysis for 3d terahertz communication systems," *IEEE Journal on Selected Areas in Communications*, vol. 39, no. 6, pp. 1817–1832, 2021. [20](#)
- [240] W. Chen, L. Li, Z. Chen, and T. Q. S. Quek, "Coverage modeling and analysis for outdoor thz networks with blockage and molecular absorption," *IEEE Wireless Communications Letters*, vol. 10, no. 5, pp. 1028–1031, 2021. [20](#)
- [241] C. Lin and G. Y. Li, "Adaptive beamforming with resource allocation for distance-aware multi-user indoor terahertz communications," *IEEE Transactions on Communications*, vol. 63, no. 8, pp. 2985–2995, 2015. [21](#)
- [242] R. Barazideh, O. Semiari, S. Niknam, and B. Natarajan, "Reinforcement learning for mitigating intermittent interference in terahertz

- communication networks,” in *Proc. of IEEE International Conference on Communications Workshops (ICC Workshops)*, 2020, pp. 1–6. **21**
- [243] A. Moldovan, P. Karunakaran, I. F. Akyildiz, and W. H. Gerstacker, “Coverage and achievable rate analysis for indoor terahertz wireless networks,” in *Proc. of IEEE International Conference on Communications (ICC)*, 2017, pp. 1–7. **21**
- [244] C.-C. Wang, X. Yao, W.-L. Wang, and J. M. Jornet, “Multi-hop deflection routing algorithm based on reinforcement learning for energy-harvesting nanonetworks,” *IEEE Transactions on Mobile Computing*, pp. 1–1, 2020. **21**
- [245] Q. Xia and J. M. Jornet, “Cross-layer analysis of optimal relaying strategies for terahertz-band communication networks,” in *Proc. of IEEE International Conference on Wireless and Mobile Computing, Networking and Communications (WiMob)*, 2017, pp. 1–8. **21**
- [246] T. Mir, M. Waqas, U. Mir, S. M. Hussain, A. M. Elbir, and S. Tu, “Hybrid precoding design for two-way relay-assisted terahertz massive mimo systems,” *IEEE Access*, vol. 8, pp. 222 660–222 671, 2020. **21**
- [247] M. Yu, A. Tang, X. Wang, and C. Han, “Joint scheduling and power allocation for 6g terahertz mesh networks,” in *Proc. of International Conference on Computing, Networking and Communications (ICNC)*, 2020, pp. 631–635. **21**
- [248] S. Nie and I. F. Akyildiz, “Beamforming in intelligent environments based on ultra-massive mimo platforms in millimeter wave and terahertz bands,” in *Proc. of IEEE International Conference on Acoustics, Speech and Signal Processing (ICASSP)*, 2020, pp. 8683–8687. **21**
- [249] C. Huang, Z. Yang, G. C. Alexandropoulos, K. Xiong, L. Wei, C. Yuen, Z. Zhang, and M. Debbah, “Multi-hop ris-empowered terahertz communications: A drl-based hybrid beamforming design,” *IEEE Journal on Selected Areas in Communications*, pp. 1–1, 2021. **21**
- [250] Q. Xia and J. M. Jornet, “Routing protocol design for directional and buffer-limited terahertz communication networks,” in *Proc. of IEEE International Conference on Communications (ICC)*, 2020, pp. 1–7. **21**
- [251] S. Javadi, Z. Wu, H. Fahim, M. M. S. Fareed, and F. Javed, “Exploiting temporal correlation mechanism for designing temperature-aware energy-efficient routing protocol for intrabody nanonetworks,” *IEEE Access*, vol. 8, pp. 75 906–75 924, 2020. **21**
- [252] N. Akkari, P. Wang, J. M. Jornet, E. Fadel, L. Elrefaie, M. G. A. Malik, S. Almasri, and I. F. Akyildiz, “Distributed timely throughput optimal scheduling for the internet of nano-things,” *IEEE Internet of Things Journal*, vol. 3, no. 6, pp. 1202–1212, 2016. **21**
- [253] F. Lemic, C. Han, and J. Famaey, “Idling energy modeling and reduction in energy harvesting terahertz nanonetworks for controlling software-defined metamaterials,” *IEEE Journal on Emerging and Selected Topics in Circuits and Systems*, vol. 10, no. 1, pp. 88–99, 2020. **21**
- [254] Q. Xia and J. Jornet, “Multi-hop Relaying Distribution Strategies for Terahertz-band Communication Networks: A Cross-layer Analysis,” to appear in *IEEE Transactions on Wireless Communications*, 2022. **22**
- [255] Z. Chen, X. Ma, B. Zhang, Y. Zhang, Z. Niu, N. Kuang, W. Chen, L. Li, and S. Li, “A survey on terahertz communications,” *China Communications*, vol. 16, no. 2, pp. 1–35, 2019. **22**
- [256] C. Jastrow, K. Munter, R. Piesiewicz, T. Kurner, M. Koch, and T. Kleine-Ostmann, “300 ghz transmission system,” *Electronics Letters*, vol. 44, no. 3, pp. 213–214, 2008. **22**
- [257] C. Jastrow, S. Priebe, B. Spitschan, J. Hartmann, M. Jacob, T. Kurner, T. Schrader, and T. Kleine-Ostmann, “Wireless digital data transmission at 300 ghz,” *Electronics Letters*, vol. 46, no. 9, pp. 661–663, 2010. **22**
- [258] H.-J. Song, K. Ajito, A. Wakatsuki, Y. Muramoto, N. Kukutsu, Y. Kado, and T. Nagatsuma, “Terahertz wireless communication link at 300 ghz,” in *Proc. of IEEE International Topical Meeting on Microwave Photonics*, 2010, pp. 42–45. **22**
- [259] H.-J. Song, K. Ajito, Y. Muramoto, A. Wakatsuki, T. Nagatsuma, and N. Kukutsu, “24 gbit/s data transmission in 300 ghz band for future terahertz communications,” *Electronics Letters*, vol. 48, no. 15, pp. 953–954, 2012. **22**
- [260] L. Moeller, J. Federici, and K. Su, “2.5 gbit/s duobinary signalling with narrow bandwidth 0.625 terahertz source,” *Electronics letters*, vol. 47, no. 15, pp. 856–858, 2011. **22**
- [261] I. Kallfass, J. Antes, T. Schneider, F. Kurz, D. Lopez-Diaz, S. Diebold, H. Massler, A. Leuther, and A. Tessmann, “All active mmic-based wireless communication at 220 ghz,” *IEEE Transactions on Terahertz Science and Technology*, vol. 1, no. 2, pp. 477–487, 2011. **22**
- [262] J. Antes, S. Koenig, A. Leuther, H. Massler, J. Leuthold, O. Ambacher, and I. Kallfass, “220 ghz wireless data transmission experiments up to 30 gbit/s,” in *Proc. of IEEE/MTT-S International Microwave Symposium Digest*, 2012, pp. 1–3. **22**
- [263] S. Koenig, D. Lopez-Diaz, J. Antes, F. Boes, R. Henneberger, A. Leuther, A. Tessmann, R. Schmogrow, D. Hillerkuss, R. Palmer *et al.*, “Wireless sub-thz communication system with high data rate,” *Nature Photonics*, vol. 7, no. 12, pp. 977–981, 2013. **22**
- [264] I. Kallfass, F. Boes, T. Messinger, J. Antes, A. Inam, U. Lewark, A. Tessmann, and R. Henneberger, “64 gbit/s transmission over 850 m fixed wireless link at 240 ghz carrier frequency,” *Journal of Infrared, millimeter, and terahertz waves*, vol. 36, no. 2, pp. 221–233, 2015. **22**
- [265] W. R. Deal, T. Foster, M. B. Wong, M. Dion, K. Leong, X. B. Mei, A. Zamora, G. Altvater, K. Kanemori, L. Christen *et al.*, “A 666 ghz demonstration crosslink with 9.5 gbps data rate,” in *Proc. of 2017 IEEE MTT-S International Microwave Symposium (IMS)*. IEEE, 2017, pp. 233–235. **22**
- [266] C. Belem-Goncalves, E. Lacombe, V. Gidel, C. Durand, F. Giansello, D. Gloria, C. Luxey, and G. Ducournau, “300 ghz quadrature phase shift keying and qam16 56 gbps wireless data links using silicon photonics photodiodes,” *Electronics Letters*, vol. 55, no. 14, pp. 808–810, 2019. **22**
- [267] S. Jia, X. Pang, O. Ozolins, X. Yu, H. Hu, J. Yu, P. Guan, F. Da Ros, S. Popov, G. Jacobsen *et al.*, “0.4 thz photonic-wireless link with 106 gb/s single channel bitrate,” *Journal of Lightwave Technology*, vol. 36, no. 2, pp. 610–616, 2018. **22**
- [268] S. Jia, L. Zhang, S. Wang, W. Li, M. Qiao, Z. Lu, N. Ideer, X. Pang, H. Hu, L. K. Oxenl *et al.*, “Ps-64qam-ofdm thz photonic-wireless transmission with 2×300 gbit/s line rate,” in *Proc. of Conference on Lasers and Electro-Optics (CLEO)*. IEEE, 2020, pp. 1–2. **22**
- [269] X. Li, J. Yu, K. Wang, M. Kong, W. Zhou, Z. Zhu, C. Wang, M. Zhao, and G.-K. Chang, “120 gb/s wireless terahertz-wave signal delivery by 375 ghz-500 ghz multi-carrier in a 2×2 mimo system,” *Journal of Lightwave Technology*, vol. 37, no. 2, pp. 606–611, 2019. **22**
- [270] C. Wang, J. Yu, X. Li, P. Gou, and W. Zhou, “Fiber-thz-fiber link for thz signal transmission,” *IEEE Photonics Journal*, vol. 10, no. 2, pp. 1–6, 2018. **22**
- [271] H. Song, H. Hamada, and M. Yaita, “Prototype of kiosk data downloading system at 300 ghz: Design, technical feasibility, and results,” *IEEE Communications Magazine*, vol. 56, no. 6, pp. 130–136, 2018. **22**
- [272] K. Nallappan, H. Guerboukha, C. Nerguizian, and M. Skorobogatiy, “Live streaming of uncompressed hd and 4k videos using terahertz wireless links,” *IEEE Access*, vol. 6, pp. 58 030–58 042, 2018. **22**
- [273] P. Sen, D. A. Pados, S. N. Batalama, E. Einarsson, J. P. Bird, and J. M. Jornet, “The TeraNova platform: An integrated testbed for ultra-broadband wireless communications at true Terahertz frequencies,” *Computer Networks*, vol. 179, p. 107370, 2020. **22**
- [274] P. Sen, V. Ariyaratna, A. Madanayake, and J. M. Jornet, “A versatile experimental testbed for ultrabroadband communication networks above 100 ghz,” *Computer Networks*, vol. 193, p. 108092, 2021. **22**
- [275] Ultrabroadband Nanonetworking Laboratory, “RED (2021) – Public Release of Data Signals for Terahertz Communication Research,” https://unlab.tech/nano_projects/red-2021-public-release-of-data-signals-for-terahertz-communications-research-and-study/, August 2021. **23**
- [276] National Instruments, “Creating a Sub-Terahertz Testbed with the NI mmWave Transceiver System,” <https://www.ni.com/en-us/innovations/white-papers/19/creating-sub-terahertz-testbed-with-ni-mmwave-transceiver-system.html>, September 2019. **23**
- [277] Keysight, “A New Sub-Terahertz Testbed for 6G Research,” <https://www.keysight.com/us/en/assets/7120-1082/white-papers/A-New-Sub-Terahertz-Testbed-for-6G-Research.pdf>, 2020. **23**
- [278] “VDI compact transmitter and receiver modules,” <https://www.vadiodes.com/>, accessed: 2021-09-30. **23**
- [279] C. He, Y. Hu, Y. Chen, and B. Zeng, “Joint power allocation and channel assignment for noma with deep reinforcement learning,” *IEEE Journal on Selected Areas in Communications*, vol. 37, no. 10, pp. 2200–2210, 2019. **23**
- [280] B. K. Jung, C. Herold, J. M. Eckhardt, and T. Kürner, “Link-level and system-level simulation of 300 ghz wireless backhaul links,” in *Proc. of International Symposium on Antennas and Propagation (ISAP)*, 2021, pp. 619–620. **23**
- [281] D. He, K. Guan, A. Fricke, B. Ai, R. He, Z. Zhong, A. Kasamatsu, I. Hosako, and T. Kürner, “Stochastic channel modeling for kiosk applications in the terahertz band,” *IEEE Transactions on Terahertz Science and Technology*, vol. 7, no. 5, pp. 502–513, 2017. **23**
- [282] S. Tarboush, H. Sarieddeen, H. Chen, M. H. Loukil, H. Jemaa, M. S. Alouini, and T. Y. Al-Naffouri, “Teramimo: A channel simulator for wideband ultra-massive mimo terahertz communications,” *arXiv preprint arXiv:2104.11054*, 2021. **23**

- [283] ThoR, “Deliverable D6.2, Concept for Software Simulation,” https://thorproject.eu/wp-content/uploads/2019/07/ThoR_TUBS_190620_D_WP6-D6.2-Software-simulation-concepts.pdf, 2019. 23
- [284] G. Piro, L. A. Grieco, G. Boggia, and P. Camarda, “Nano-sim: simulating electromagnetic-based nanonetworks in the network simulator 3.” in *Proc. of SimuTools*, 2013, pp. 203–210. 23
- [285] Z. Hossain, Q. Xia, and J. M. Jornet, “TeraSim: An ns-3 extension to simulate Terahertz-band communication networks,” *Elsevier Nano Communication Networks Journal*, vol. 17, pp. 36–44, 2018. 23
- [286] A. A. Gargari, M. Polese, and M. Zorzi, “Full-stack comparison of channel models for networks above 100 ghz in an indoor scenario,” *arXiv preprint arXiv:2110.06838*, 2021. 23